ORNL/TM-2022/2377

Simplified High-Temperature Molten Salt CSP Plant Preconceptual Design

Kevin R. Robb

March 2022

OAK RIDGE National Laboratory

ORNL IS MANAGED BY UT-BATTELLE LLC FOR THE US DEPARTMENT OF ENERGY

ORNL/TM-2022/2377

Nuclear Energy and Fuel Cycle Division

SIMPLIFIED HIGH-TEMPERATURE MOLTEN SALT CSP PLANT PRECONCEPTUAL DESIGN

Kevin R. Robb

March 2022

Prepared by
OAK RIDGE NATIONAL LABORATORY
Oak Ridge, TN 37831
managed by
UT-BATTELLE, LLC
for the
US DEPARTMENT OF ENERGY
under contract DE-AC05-00OR22725

CONTENTS

LIST OF FIGURES v
LIST OF TABLES v
ABBREVIATIONS vi
ACKNOWLEDGMENTS vii
ABSTRACT 1
1. CONCEPT OVERVIEW 1
1.1 BACKGROUND 1
1.1.1 Current State-of-the-Art and Challenges 1
1.1.2 Next Generation Technology and Challenges 2
1.2 BASELINE CONCEPT INTRODUCTION AND LAYOUT 3
1.2.1 Thermocline and Tank 6
1.2.2 Material Selection 7
1.2.3 Baffle 9
1.2.4 Salt-to-sCO_2 Heat Exchanger 9
1.2.5 Riser Pipe 10
1.2.6 Pump and Sump Tank 11
1.2.7 Receiver 11
1.2.8 Thermal Muffler 12
1.2.9 Tower: Thermocline Tank Structural Support 12
1.2.10 Ullage Gas Control System 13
1.2.11 Salt Chemistry Control 13
1.2.12 Salt Flow Control across Heat Exchanger 13
1.2.13 Operation Instrumentation and Control 14
1.2.14 Solar Reflector Field 15
1.2.15 sCO_2 Power Block 15
1.2.16 Site Configuration and Scale-Up 16
1.2.17 Design Alternatives 16
1.3 SUMMARY COMPARISON TO EXISTING PLANTS 20
2. CHLORIDE SALT SYSTEM POINT DESIGNS 21
2.1 0-D DESIGN AND ANALYSIS METHODS 21
2.1.1 Applicable Standards 21
2.1.2 Material Properties 21
2.1.3 Weighted Cost Metric and Value Metric 22
2.1.4 Thermocline Vessel Shell, Top Head, and Bottom Head 22
2.1.5 Vessel Insulation and Heat Loss 23
2.1.6 Baffle 24
2.1.7 HCHX 25
2.1.8 Sump Tank 26
2.1.9 Vessel Flange 26
2.1.10 Design Criteria and Constraints for point designs 26
2.2 EXAMPLE DESIGN SCOPING RESULTS 26
2.2.1 Additional Sensitivities for 5 MW_t System 30
2.3 POINT DESIGN FOR 5 MWT WITH 12 HOUR TES 35
2.3.1 Bill of Materials for Point Design 38
3. NITRATE SALT SYSTEM POINT DESIGN 40
3.1 INTRODUCTION 40
3.2 METHODOLOGY 40
3.3 RESULTS AND COMPARISON TO CHLORIDE SALT POINT DESIGN 40

4. DEVELOPMENT ROADMAP 44
4.1 CONCEPT MATURATION 44
4.1.1 Subcomponent Analysis, Design, and Demonstration 44
4.1.2 Detailed Plant Modeling 44
4.1.3 Detailed System Conceptual Design 44
4.2 1-5 MW_t DEMONSTRATION 44
4.3 PILOT PLANT 45
5. REFERENCES 46
APPENDIX A. SUPPLEMENTAL INFORMATION A-1
A.1 CHLORIDE SALT 5 MW_T SYSTEM DESIGN MODEL DETAILS A-2
A.2 NITRATE SALT 5 MW_T SYSTEM DESIGN MODEL DETAILS A-7

LIST OF FIGURES

Figure 1. Illustration of a two-tank power-tower CSP plant [3]. 2
Figure 2. Schematic of proposed concept. 5
Figure 3. Example plant layout of modular units with shared power cycle. 16
Figure 4. Alternate layout 1. 17
Figure 5. Alternate layouts 2 and 3. 18
Figure 6. Variation of thermocline tank weight for various point designs. 29
Figure 7. Variation in weighted cost metric for various point designs. 29
Figure 8. Variation in value metric for various point designs. 30
Figure 9. Variation in value metric–to–tank L/D ratio. 31
Figure 10. Variation on system dimensions with tank L/D ratio. 31
Figure 11. Required system gas pressure for various tank L/D ratios. 32
Figure 12. Value metric vs. outer insulation thickness. 33
Figure 13. Variation of HCHX tube bundle. 34
Figure 14. Variation on value metric with system maximum temperature variations. 35
Figure A.1. Concept schematic with dimension notations. A-1

LIST OF TABLES

Table 1. Molten salt thermocline experimental studies without filler 6
Table 2. Instrumentation suite 15
Table 3. Assumed salt properties for sizing analysis 21
Table 4. Assumed material density and prices for cost metric 22
Table 5. Summary of nonoptimized systems 28
Table 6. Summary point design 36
Table 7. Detailed estimate of component masses and material costs 37
Table 8. Major component mass and cost fraction 37
Table 9. Raw material mass, mass fraction, and cost fraction 38
Table 10. Value metric for alternate cost model 38
Table 11. Assumed material densities and prices for the nitrate system cost metric 40
Table 12. Summary point design for nitrate system 41
Table 13. Detailed estimate of component masses and material costs for nitrate system 43
Table 14. Major component mass and cost fraction for nitrate system 43

ABBREVIATIONS

API	American Petroleum Institute
ASME	American Society of Mechanical Engineers
AWWA	American Water Works Association
BPVC	Boiler and Pressure Vessel Code
CSP	concentrating solar power
DOE	US Department of Energy
EERE	Office of Energy Efficiency and Renewable Energy
HCHX	helical coil heat exchanger
HTF	heat transfer fluid
ID	inner diameter
OD	outer diameter
ORNL	Oak Ridge National Laboratory
STEP	Supercritical Transformational Electric Power
TES	thermal energy storage

ACKNOWLEDGMENTS

This material is based upon work supported by the U.S. Department of Energy's Office of Energy Efficiency and Renewable Energy (EERE) under Solar Energy Technologies Office (SETO) Agreement Number 37367.

ABSTRACT

State-of-the-art, concentrating solar power plants generally rely on a two-tank system with a large central tower. These plants employ nitrate salts that are limited to approximately 565°C, in practice. A novel system arrangement is proposed using molten salt as the heat transfer and energy storage medium in a single thermocline storage tank with an integral heat exchanger to the power cycle. The system's unique features enable temperatures higher than 565°C while reducing costs. This study explores the considerations for the concept and presents a preconceptual point design for a 5 MW_t system capable of generating 100 MW_t per day with 12 hours of thermal energy storage. This study also examines the potential operation of the system with nitrate and higher temperature chloride salts. Both salt systems appear promising, and future concept maturation is recommended.

1. CONCEPT OVERVIEW

1.1 BACKGROUND

1.1.1 Current State-of-the-Art and Challenges

Concentrating solar power (CSP) plants focus the sun's energy to a heat transfer fluid (HTF) and convert the thermal energy to electricity. As of 2018, numerous CSP plants are in operation (98), under construction (18), and under development (24) worldwide [1]. There are two main types of CSP plants in operation: the parabolic trough configuration and the power tower configurations. For the solar power tower configuration shown in Figure 1, the HTF and thermal energy storage (TES) media are pumped from a large cold TES tank, up a tower, to a central receiver. A field of heliostats on the ground directs sunlight onto the receiver to heat the HTF. The hot HTF is then transferred to and stored in a large hot TES tank. After it passes through a heat exchanger, hot HTF can then be pumped back to the cold tank on demand. The heat exchanger supplies energy to drive a power cycle. Current state-of-the-art CSP plants use nitrate/nitrite-based salts and a steam Rankine power conversion cycle. The salt is used as both the HTF and the TES media. In practice, nitrate salts are limited to peak temperatures of 565°C. For scale, plants under development are in the 50–450 MW_e range [2], with tower heights on the order of 140–200 m.

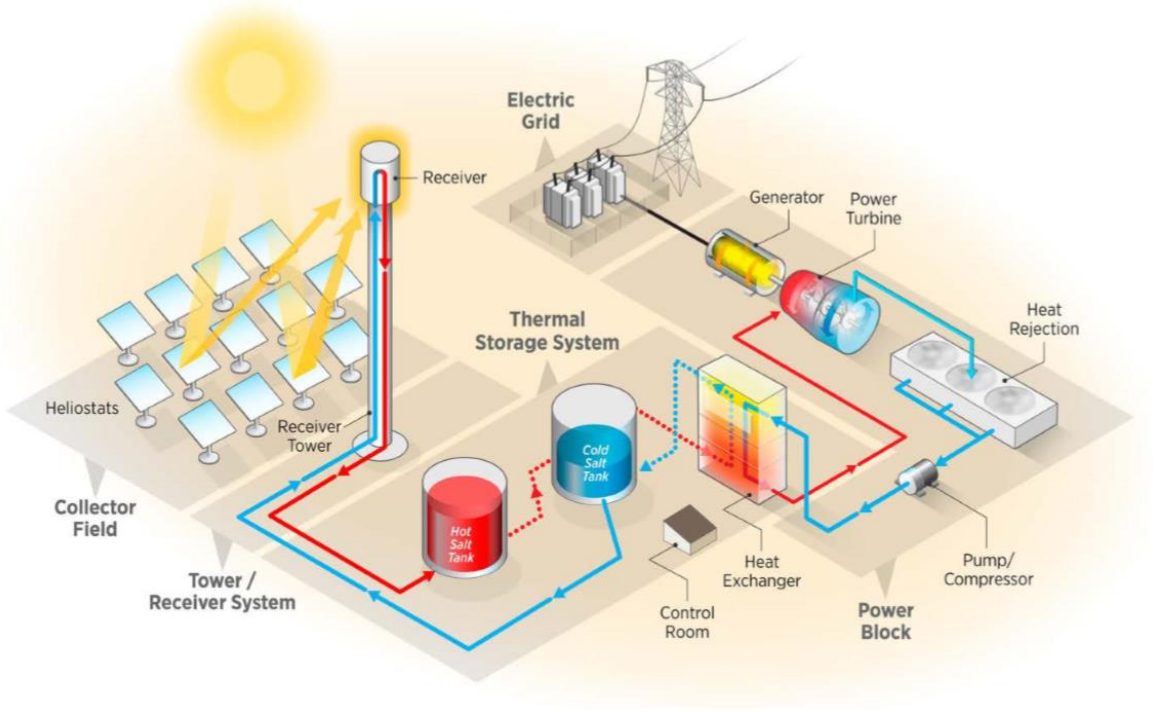

Figure 1. Illustration of a two-tank power-tower CSP plant [3].

Salt-based CSP systems with TES have a few technical challenges. Power tower systems require a high-head pump to initially push the TES media up the tower to the receiver. Whereas this high-head pump is on the *cold* side of the system, temperatures are still elevated, so the service conditions require a specialized pump. Long runs of hot-side and cold-side piping are typically required between the receiver, TES tanks, and power conversion cycle. In addition to the required piping, supports, and thermal expansion accommodation, these pipe sections require trace heating, insulation, and monitoring. For the two-tank system, the thermal expansion of the TES tanks is an engineering challenge. Although large tanks are used in many industries (e.g., petrochemical), the relatively large thermal expansion experienced by the tanks under the high-temperature operation is unique and presents a challenge. Many of these challenges are captured in a recent study of industry experience with molten salt power tower systems. The study [4] results summarize five general topic areas of challenges:

1. Leaks in hot salt tanks
2. Leaks in salt steam generators
3. Differences between actual and expected site radiation
4. Differences between actual and expected flux distributions on the receiver
5. Heat trace capacity and insulation quality

1.1.2 Next Generation Technology and Challenges

The US Department of Energy (DOE) Office of Energy Efficiency and Renewable Energy (EERE) is focused on developing the next generation of CSP technology: Gen3 CSP. These systems will operate at higher temperatures with improved economics [3]. Chloride and carbonate molten salts are candidate HTF and TES media. Because of the comparatively high cost of carbonate salts, chloride salts are a leading candidate for HTF and TES. The hot sides of these systems will operate at temperatures exceeding 725°C to enable the efficient use of supercritical carbon dioxide (sCO_2) power cycles boasting high thermal efficiencies.

As noted in the 2017 Gen3 CSP roadmap, several challenges must be addressed before the demonstration and widespread deployment of Gen3 molten-salt based CSP technology. To inhibit corrosion, chloride salts must remain devoid of moisture. This requires the use of an inert cover gas, a relatively hermetic system, and monitoring of the salt condition. In addition to corrosion resistance, the salt-wetted materials must also have suitable high-temperature properties (i.e., strength, creep, fatigue, and air oxidation resistance). At this writing, the commercial supply chain for high-temperature molten salt components (e.g., pumps, valves, flanges, tanks, and heat exchangers) is very limited. Efforts are underway to develop and demonstrate component performance and establish a supply chain. Beyond the upfront construction costs, component and system reliability are important factors that impact the operation and maintenance (O&M) costs for CSP plants.

A 1 MW_t integrated demonstration system was recently proposed to de-risk and demonstrate the technology for Gen3 CSP plants [5]. The demonstration system used chloride molten salt TES in a two-tank system and a liquid metal sodium HTF at the receiver. The extensive project made several advancements in chloride salt plant design and its underlying technologies. A risk registry was developed which noted the following significant risks:

1. tank liner integrity
2. salt valve performance
3. salt vapor impacts on system components
4. salt piping freeze recovery
5. pressure and chemical sensor performance
6. online corrosion control
7. sodium-alloy 740H alloy compatibility
8. sodium fires

The higher operating temperature of next-generation system enables the use of sCO_2 power cycles. These cycles enable high-efficiency power conversion with compact components. Several DOE and industrial-led efforts are under way to develop the sCO_2 power cycle. The Supercritical Transformational Electric Power (STEP) program is working to develop and demonstrate a power cycle of approximately 10 MW_e (i.e., approximately 23 MW_t) [6]. A separate program supported by the European Union, sCO_2flex, is focused on the design and validation of a 25 MW_e power cycle [7]. Other than these projects, universities continue to make focused contributions to the technology, and several companies are working to develop and commercialize sCO_2 power cycles.

1.2 BASELINE CONCEPT INTRODUCTION AND LAYOUT

The promise and challenges associated with existing and future molten salt–based CSP plants were briefly summarized in Section 1.1. This study's objective was to create a simplified high-temperature molten salt–based Gen3 CSP concept with TES. The overall design goals for the concept are as follows:

1. limiting technical risk
2. lowering construction costs
3. reducing operation costs

Efforts to realize the goals include the following:

1. Reduce the number of components
2. Reduce and simplify the engineering challenges of components
3. Utilize lower cost materials by reducing the area in contact with high-temperature salt
4. Simplify onsite construction

5. Reduce and simplify required operation and maintenance activities

The concept developed and described herein revolves around a single thermocline tank using molten chloride salt as the HTF and TES media, as shown in Figure 2. A salt sump tank is located above the thermocline energy storage tank. Elevated pressure of the ullage gas in the top of the thermocline tank forces cold salt from the bottom of the thermocline, through a riser, and into the sump tank. A pump takes suction from the sump tank and forces the HTF through a receiver, and then it returns the hot salt into the top of the thermocline tank. An insulated baffle within the thermocline tank creates an outer annulus which houses a salt-to-sCO_2 helical coil heat exchanger (HCHX). The temperature-driven density difference of the salt in the inner region and the annular region creates a differential driving pressure to force hot salt down through the heat exchanger. The flow of salt through the HCHX is regulated as the thermocline moves axially along the inner region of the tank during charging and discharging.

The focus of this study is to develop a preconceptual design of the system. The remainder of Section 1 describes the design considerations and components in more detail. This study focuses on the unique attributes of the proposed concept. The design and detailed modeling of the reflector field and power cycle are outside the scope. However, the interface between the proposed concept and these systems are accounted for and discussed. Section 2 presents a scoping assessment of system sizing. A point design is downselected and presented. Sections 1 and 2 are focused on high-temperature chloride salt-based systems. Modification of the proposed concept for use with nitrate salts is explored in Section 3, with example calculations. The maturity of the proposed concepts will be demonstrated in the preconceptual designs. As such, the concept requires additional effort to mature. Areas that require future development and a potential maturation path are discussed in Section 4.

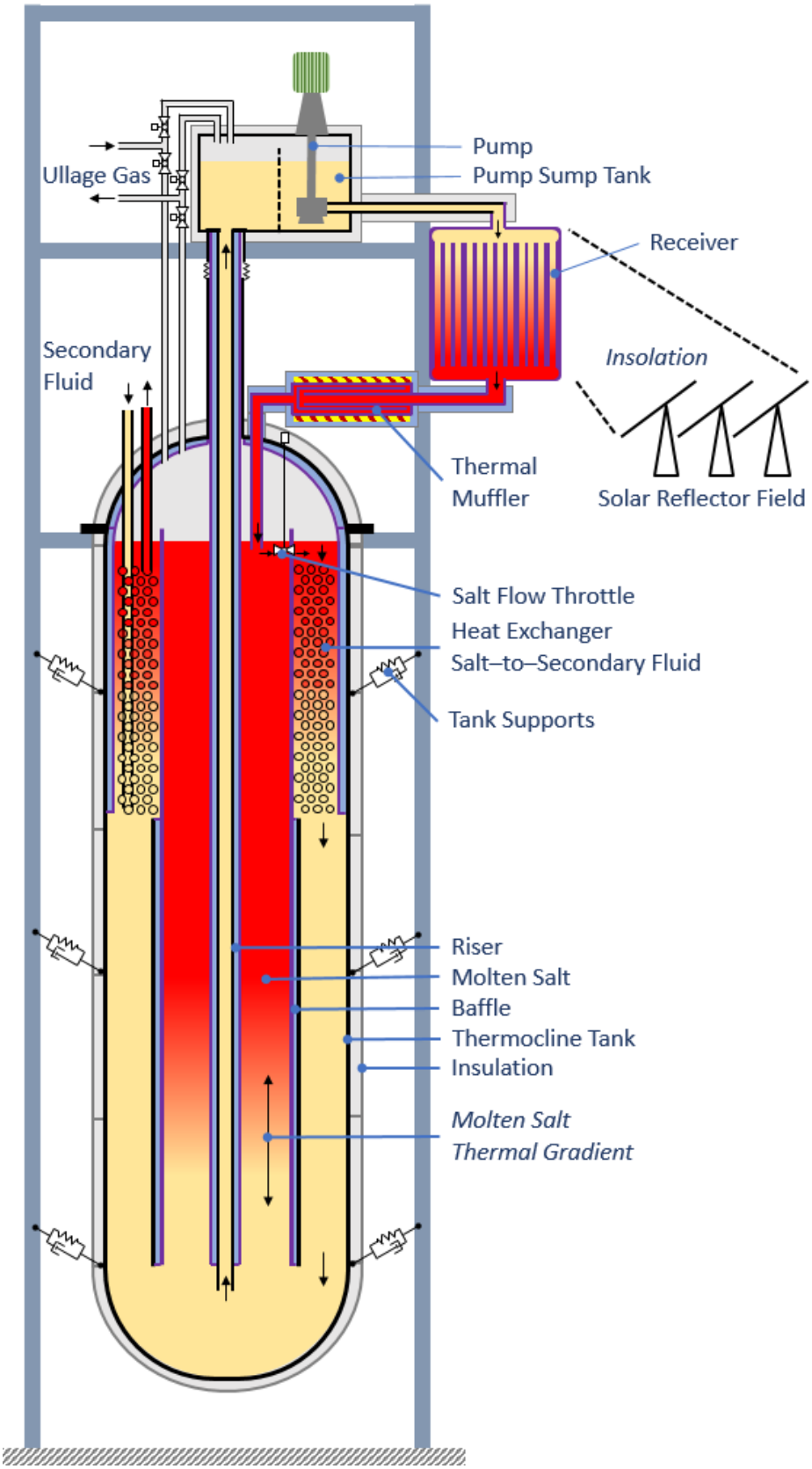

Figure 2. Schematic of proposed concept.

1.2.1 Thermocline and Tank

Thermocline stability is a key consideration for this concept. For nitrate salt systems, filler materials such as various rocks or sand are substantially cheaper than the nitrate salt [9, 10]. Therefore, most thermocline stability studies for molten salt systems to date have included filler material. Because the cost of chloride salt is low and the salt itself is an excellent TES media, the current concept excludes filler material. This prevents issues associated with thermal ratcheting (i.e., a detrimental phenomenon caused by the filler material). Limited experimental data without filler has been developed for nitrate-based salt thermoclines, as shown in Table 1. Within the bounds of this limited dataset, the single-media nitrate salt thermocline is shown to be stable. However, these data are for systems smaller than those considered in this study, they capture a limited range of operational conditions, and they are not for chloride salts. As discussed in Section 4.1, thermocline stability must be tested and analyzed for further concept maturation.

Table 1. Molten salt thermocline experimental studies without filler

Study	Salts	Thermal capacity (MWh)	Tank ID (m)	Tank length (m)	Flow rate (mm/s)
Seubert et al., 2017 [8]	Solar salt	0.72	0.591[a]	1.3	0.4[b]
Ho Kim et al., 2019 [10]	Solar salt and HITEC	0.80	0.6	1.5	0.09–0.19[c]
Odenthal et al., 2018 [11]	Solar salt	4	1.1	5.4	0.5[b]

[a] Assuming the DN600 pipe was schedule 40
[b] Estimated based on experiment data presented for thermocline discharge time
[c] Estimated based on experiment mass flow rate, density of hot salt, and tank inner diameter (ID)

Because of the unique design, the thermocline tank pressure boundary is exposed only to “cold” salt. At the cooler temperature, the salt corrosion kinetics are slower, and containment materials have higher strength and creep resistance. This enables the use of less expensive materials (i.e., stainless steels rather than superalloys) and thinner tank walls. The lower temperature wall also reduces external thermal energy losses and the need for insulation.

Depending on state regulations and trucking routes, domestic ground shipping widths of 12.5, 14.5, and 16 feet (3.8–4.9 m), and potentially larger, are attainable. Weight limits are influenced by the route. As demonstrated in Section 2.2, the outer diameter (OD) of the thermocline can be sized to enable ground transport. This enables most tank fabrication to be conducted at an offsite fabrication facility, and the modular sections can be shipped thus reducing costs and affording greater quality control.

Length must also be considered for the ground shipment scenario, but this factor much less constraining than width. Except for sub-megawatt sized systems, the tank would need to be shipped in segments and then assembled onsite using flanges or welding. Flanges require bolting and seals, as well as additional bulk metal and machining. Flanges are also potential leakage points. However, if sections are welded sections together onsite, additional highly skilled workers and inspection will be required. Because the tank uses common materials such as stainless steel rather than super alloys, the benefits of a welded tank should outweigh those of a bolted design. Therefore, the tank is assumed to be welded together except for one flange connection at the top to facilitate maintenance and inspection of the HCHX. Ultimately, this design decision would be informed through an economic and risk analysis.

Oil atmospheric distillation columns have a similar size to the envisioned thermocline tank. These vertically mounted columns operate at elevated temperatures, and although they are near atmospheric pressure, they are pressurized. The largest column, which was shipped as a single unit, was installed at

Nigeria's Dangote Refinery and is 112 m long, 12 m in diameter, and it weighs 2,252 tons [13]. Based on these comparable factors, the refining industry's experience base and supply chain support the feasibility of the proposed concept.

The relatively low temperature insulation and trace/guard heating on the outside of the tank are standard industrial items that would be selected based on an economic trade-off study. Representative insulation choices considered in this study are discussed in Section 1.2.2.

1.2.2 Material Selection

A host of considerations applies to material selection, including their mechanical properties, cost, supply chain, the specifics of code acceptance, salt compatibility, fabricability, and others. One possible solution may be to use a 300 series stainless steel for the cooler sections and a higher nickel alloy for the hot sections. For the purposes of this preconceptual design, a subset of materials was considered. Further refinement of material selection and techno-economic optimization of the concept are left for future work.

1.2.2.1 Cold wall material

A key feature of the proposed design is the reduced demands on the system's boundary materials. The lower temperatures (e.g., 500–600°C) to which the materials are exposed result in higher strength and creep resistance, as well as lower corrosion rates. These factors facilitate the use of stainless steels in the pressure boundary. Stainless steel alloys 304, 316, and 347 are reasonable candidates given their material properties, availability, and code acceptance. For high-temperature application, codes generally require the higher carbon content specification for the alloys (i.e., 304H, 347H, 316H) or material analysis demonstrating ≥0.04% carbon content. For example, the American Society of Mechanical Engineers (ASME) Boiler and Pressure Vessel Code (BPVC) requires the higher carbon content in all three alloys for applications above 550°C. This is near the anticipated cold-side temperature of the system. The simplicity of the proposed design relies on plate forms of the alloys. It would likely be easier to source the higher carbon content versions of the alloys in plate form than other product forms. There are additional considerations for selecting the alloy for the cold-side. For example, the material's allowed stresses can depend on the application's amount of permanent strain tolerance and may be time dependent (e.g., creep phenomena). Finally, although corrosion rates are lower at lower temperatures, the corrosion resistance of the alloys at lower temperatures (e.g., 500–600°C) has not been explored as much as that for higher temperatures. Evaluating the long-term lower temperature corrosion rates may be an area for future study. Given these considerations, alloys 304, 347, and 316 with carbon contents ≥0.04% were considered for the "cold" structural material.

1.2.2.2 Hot wall material

Whereas stainless steels can be used at high temperatures, nickel-based superalloys have been designed with improved characteristics such as creep resistance for such applications. In addition, high-nickel alloys have demonstrated improved corrosion resistance in molten salt environments. However, raw material and fabrication are much more expensive for high-nickel alloys. In keeping with the design goal to limit costs, this concept intentionally minimizes the use of high nickel alloys. Features in contact with the high-temperature salt include the HCHX, receiver and limited piping. Depending on the design, the baffle (see Section 1.2.3) may also include a high-nickel alloy that is in contact with the hot salt. As pressure boundaries for the system, the HCHX, receiver, and some piping will likely require applicable code-qualified materials such as alloys 617, 625, 230, 800H, X, or 601. Inconel® alloy 740H®, Haynes® 282® and a range of other newer advanced alloys may be applicable, but they are at various stages of code acceptance and industrial adoption. However, many of these alloys for high-temperature application contain an appreciable amount of chrome (i.e., >20%). Molten halide salts are known to preferentially

attack chrome in alloys. Alloy N is a high-temperature nickel-based low-chromium alloy that was designed specifically for molten salt service. However, its code acceptance is limited and only extends to 704°C (e.g., for ASME BPVC VIII-1). A newer generation of alloys with improved mechanical properties, good halide compatibility, and low chrome content (e.g., Haynes® 242®, Haynes® 244®) currently do not have the requisite code acceptance. Finally, two other alloys, 600 and C-276, are widely available commercially, have moderate chromium concentrations (i.e., 14–17%), and have a wide range of code acceptance, but not up to the temperatures envisioned for the hot side (i.e., >700°C). Given all these considerations alloys 617, 625, and 230 were included in the preconceptual design for the hot service material.

1.2.2.3 External insulation

Outside the system, standard high-temperature industrial insulation could be used. Two representative insulations were considered: a mineral wool (e.g., ProRox® MA 960NA [18]) and a higher performance aerogel-based insulation (e.g., Pyrogel® XTE [19]).

1.2.2.4 Internal insulation

Two possible configurations are envisioned for insulation inside the system. The insulation is either hermetically encased (e.g., within metal sheathing), or it is in contact with the salt. Key considerations for the insulation are as follows:

- Chemical compatibility (for salt contacting insulation option)
- Thermal conductivity
- Density
- Cost

For the proposed concept, it is advantageous to reduce the volume of insulation inside the vessel because it displaces the TES salt. While this is also the case for a ground-based tank, this factor is more important for the proposed concept because of the lower ratio of salt volume to tank surface area (i.e., there is more surface area to lose heat per unit volume of stored energy). It is also advantageous to decrease the overall weight of the insulation as the tank for the proposed concept is suspended.

Insulation contacting the salt faces several challenges. The chemical compatibility of salt with insulating materials (e.g., silica, alumina, zirconia, magnesia, calcium silicate, aluminosilicate) has been analyzed less in the literature than for alloys. Beyond the compatibility of the base material, many insulations rely on trapped air to reduce thermal conductivity. Air is known to be detrimental to salt compatibility. Air in interconnected porosity, and most likely closed porosity, would need to be replaced with an inert gas or vacuum. The thermal conductivity of chloride salt is on the order of 0.4–0.5 W/m K [20], which is higher than many desirable insulating materials. Therefore, low permeability (e.g., closed cell) insulations must be used if salt is anticipated to be in contact with the insulation. The thermal conductivities of many dense refractory materials are quite high. Whereas forsterite (magnesium silicate), cordierite, and mullite may be compatible with hot chloride salt [21, 22, 23], their thermal conductivities are all greater than 1 W/m K (i.e., higher than the salt), and their densities greater than 2 g/cc. Although salt-contacting insulation may be a reasonable option for ground-based tanks, a more compact, lightweight option will likely be required for the proposed concept.

A hermetically sealed insulation that is sandwiched and sealed between metal sheathing is an attractive option. To mitigate the impact of a possible leak through the sheathing, the air trapped inside should be replaced with an inert gas or vacuum. While the top of the vessel operates at low pressures (e.g., 200 kPa) the hydrostatic pressure lower in the vessel can be significant. Designing an insulation structure to

maintain vacuum conditions at high temperatures within the system is a challenge. Backfilling the insulation with an inert gas appears to be more practical solution and was pursued further for this preconceptual design. A range of possible insulation materials were considered, including those based on alumina, silica magnesia, mineral wool, aerogel, and microporous technology.

Ultimately, microporous insulation was chosen because of its superior thermal resistance. Microporous insulation contains pores smaller than the mean free path of the gas to inhibit convective heat transfer, and it can contain opacifiers to inhibit thermal radiation heat transfer through the material. These properties result in very low effective thermal conductivity values for microporous insulation.

1.2.3 Baffle

An annular baffle/shroud separates the inner high-temperature thermal energy storage region and the outer annular region that houses the heat exchanger and cold salt return flow path. The shape of the baffle can be a simple uniform cylinder along the length of the tank, or the baffle could have a different diameter at the heat exchanger region than along the cold salt return path. With a fixed vessel diameter, increasing the inner area enables greater TES capacity, but this increases the resistance to flow in the annular space and reduces the maximum flow rate of salt attainable over the heat exchanger. A study using water as the working fluid found that the simple uniform cylinder geometry outperformed more complex geometries for a range of metrics [14]. In the present study, the annular space for the HCHX is sized to accommodate the HCHX, whereas the annular return path below is assumed to be a fixed size. Further refinement and optimization of the geometry may be pursued in the future.

Beyond geometry, considerations and goals for the baffle's design include the following:

- Prevention of cross flow and mixing between the inner and annular salt regions (i.e., solid)
- Thermally insulation to limit heat transfer from the hot inner region to the cold salt return
- Limited thickness of the baffle, because it displaces TES salt
- Sufficient hot- and cold-salt compatibility.
- Reasonable manufacturability and economics

The baffle must inhibit heat loss from the inner region to the annular region. As discussed in Section 1.2.2, two options were considered for the insulation. One option uses a salt-contacted refractory insulation with a single thin metal wall to prevent salt cross flow. Another option is to use either fibrous or solid insulating materials sandwiched between metal walls. Based on the considerations discussed in Section 1.2.2 and early scoping calculations, the sandwiched microporous insulation option was chosen.

Surrounding the insulation, the hot-wall metal alloy was chosen for the inner wall, because it needs to be compatible with the hot salt. The outer wall can be made of the hot- or cold-wall material. Ultimately, the cold-wall metal alloy was chosen for the outer baffle wall. Although the cold-wall alloy is significantly less expensive than the hot-wall alloy, the use of the cold-water metal alloy introduces a dissimilar weld. Another very important design consideration is the differential thermal expansion. As the system progresses from ambient to operation temperature, it undergoes significant thermal expansion. By making the outer wall of the baffle from the same material as the vessel, their thermal expansion is the same; this simplifies the design for securing the baffle.

1.2.4 Salt-to-sCO_2 Heat Exchanger

A helical coil design was chosen for the integral heat exchanger. The HCHX resides at the top of the outer annulus of the thermocline tank. sCO_2 passes through the tube coils, while salt driven by natural convection flows downward across the coils.

The HCHX is exposed to hot salt, hot sCO_2, a significant pressure differential between the sCO_2 and salt sides, and a considerable temperature differential between the inlet and outlet. A superalloy with sufficient wall thickness must be used to accommodate corrosion and to resist creep, and the mechanical design must accommodate the pressure and temperature differentials.

The HCHXs considered in this study are within the scale of those fabricated for the natural gas, gas treatment, and methanol industries [24]. They can be designed for high-temperature and high-pressure applications. The basic design of an HCHX is conducive to accommodating thermal expansion and transients. Unlike micro-channel heat exchangers, the HCHX macro-scale features are less susceptible to fowling.

Because it is located towards the top of the thermocline tank, the HCHX can be inspected by partially draining of the tank. Alternatively, if the salt is sufficiently clear, then the submerged HCHX could be visually inspected with further development of the technology. Tube failure would result in sCO_2 leakage into the salt. Small leaks from the HCHX could be detected through monitoring the salt's chemical composition. Larger leaks could be detected by the ullage gas system or through a mass balance of the sCO_2 side (e.g., monitoring the HCHX sCO_2 inlet and outlet flow rates).

If the HCHX needed to be replaced, it could be extracted from the top of the thermocline tank. This operation would require draining the tank and removing the long riser pipe. A flange on the top head of the vessel is included as part of the preconceptual design to facilitate removal. The flange, bolts, and seal located in the gas space increase system cost and weight, but a flanged connection to facilitate removal of the HCHX is likely desirable for a first-of-a-kind demonstration. A seal-welded design may have economic advantages for N^{th}-of-a-kind deployment. The trade-off between the design life and replacement of the heat exchanger would be further informed by an economic analysis.

1.2.5 Riser Pipe

The cold salt from the bottom of the thermocline tank flows to the sump tank through the riser pipe. Flow through the riser pipe is controlled via the pressure differential between the thermocline tank head space and the sump tank head space, as seen Section 1.2.10.

The riser passes through the hot salt at the top of the thermocline. The pipe and baffle share design considerations; the pipe should be insulated to prevent heat loss from the hot salt to the inner cold salt. The riser pipe could be located along the centerline of the thermocline tank, along the inside of the baffle, or in the annular space. For simplicity, the riser is assumed to be on the centerline of the thermocline tank. A symmetric system would facilitate uniform flow rates and thermocline stability. Alternative configurations for the riser pipe are discussed in Section 1.2.17.

The riser pipe is a single structure that is inserted through the bottom of the sump tank and into the thermocline tank. The pipe is mounted to and sealed against the inside surface of the sump tank. This single attachment point facilitates differential thermal expansion between the sump tank and the thermocline tank, as well as along the riser pipe itself.

Between the top of the thermocline tank and the bottom of the sump tank (i.e., outside), the riser pipe is sheathed by an outer pipe made of the low-temperature alloy. The riser is inserted through this outer pipe. To accommodate differential thermal expansion or other movement between the two tanks, the outer pipe incorporates a bellows. The outer pipe is a gaseous pressure boundary interconnected to the thermocline tank. Any leakage through the seal between the sump tank and the riser pipe would be contained within the outer pipe.

1.2.6 Pump and Sump Tank

A key benefit of the concept is that it relies on only one cold-salt low-head pump. Unlike current nitrate salt CSP power tower systems, there are no hot-salt pumps or high-head pumps in this concept. The pump can be a short-shafted, single-stage, cantilevered design, which would offer several advantages. The short-shafted design does not require molten salt–wetted bearings or seals. Although efforts are underway to develop this technology, currently there are no demonstrated bearings for chloride salt service. By not incorporating salt wetted bearings, maintenance and replacement of this wear component is precluded. This type of pump has also been used in high-temperature molten salt systems [15] and is the same type employed for the forced-flow salt loops at Oak Ridge National Laboratory (ORNL) (i.e., LSTL [16] and FASTR [17]). The short-shafted weighs less and is shorter than the long-shafted pumps, which simplifies fabrication, mounting, removal, and maintenance. The pump would be driven by a variable frequency drive (VFD), thus permitting control of the salt flow rate through the receiver.

The pump takes suction from the sump tank that is located above the thermocline tank. By maintaining the ullage gas space pressure[1] in the thermocline and sump tanks, the cold salt is pushed through the riser pipe into the sump tank. Reducing the ullage gas pressure in the top of the thermocline tank (i.e., venting) allows the sump tank and receiver to be readily drained back into the thermocline tank. The short-shafted pump design and the ability to drain the salt around the pump facilitates servicing/replacing the pump as needed.

The sump tank can be relatively small. The main requirement is to maintain a sufficient depth of salt to prevent the pump from entraining gas. The tank incorporates baffles to suppress potential sloshing and to further reduce the possibility of gas entrainment. The volume should be large enough to accommodate transient pump start/stop cycles and changes in flow rate. These transients are influenced by the momentum of salt within the system and the response time of the ullage gas system.

1.2.7 Receiver

The design and optimization of receivers for liquid HTFs have been studied extensively. The preconceptual system receiver has the same requirements as a two-tank high-temperature salt system. The receiver would be located below the discharge of the pump, above the thermocline tank, and within an insulated, heated cavity (e.g., similar to an industrial furnace). After filling the receiver with salt, the door to the cavity would be opened to allow for insolation.

During the filling process, cold salt from the bottom of the thermocline tank is pushed up through the riser pipe into the sump tank, and the hot salt is simultaneously pushed up into the receiver from the top of the thermocline tank. Thus, the receiver side of the system starts with hot salt, thus decreasing the demands of the trace heating system. Alternative configurations of the receiver location are presented in Section 1.2.17.

Because the receiver is not unique to the proposed concept, its design and optimization was excluded from the scope of this study. For the preconceptual design discussed in Section 2, a simple tube sheet with an applied heat flux was assumed for scoping purposes.

[1] The pressure is approximately equal to the salt head as measured between the salt-free surfaces in the thermocline tank and the sump tank, in addition to any overpressure of the pump sump tank ullage gas.

1.2.8 Thermal Muffler

The thermal muffler, which is located after the outlet of the receiver, helps handle salt temperature fluctuations from the receiver. During operation, fluctuations in insolation caused by clouds, cooling of the receiver by wind gusts, and other transient phenomena can impact the receiver's outlet temperature. It is desirable to maintain uniform temperatures in the hot and cold regions of the thermocline tank to promote thermocline stability. The heliostat field and VFD-controlled pump play key roles in regulating receiver outlet temperature. The thermal muffler was added to provide passive dampening of the temperature fluctuations for timescales more rapidly than the pump response time (i.e., a couple seconds). The muffler is constructed of three or more concentric pipes/tubes. The pipes are situated to create a counter current flow of the salt. Small holes between the cavities enable complete draining. Salt mixing within the component, as well as heat transfer to the adjacent counter current flow, help dampen temperature fluctuations. Furthermore, auxiliary electrical heaters on the outside shell can also be used to maintain consistent outlet temperatures. The muffler may be oversized to provide additional auxiliary system heating.

The component is simple to fabricate, install, and operate, but design optimization requires at least two-dimensional dynamic modeling, and the need for and utility of the muffler is dependent on the anticipated system transients. The component was included in the preconceptual design, but design analysis and optimization are proposed for future work.

1.2.9 Tower: Thermocline Tank Structural Support

A frame surrounds and holds the thermocline tank, sump tank, and receiver. Three concepts for supporting the tank have been developed:

1. Hangers from the frame could support the suspended thermocline tank,[2] as illustrated in Figure 2. The hangers accommodate thermal expansion of the tank, and with appropriate damping, they can be used to provide seismic resistance for the site if required. Construction of the tank could proceed from the top down or from the bottom up.

2. A large flange around the top of the tank could be set on the tower. The majority of the tank would hang down from the flange, and the tank would thermally expand downward. Construction of the tank would likely proceed from the top down.

3. A combination of options 1 and 2 could be implemented.

The foundation for the tower structure must support the load of the tower structure, salt, thermocline tank, sump tank and receiver, and it must resist overturning moments. In contrast to the foundations used for the existing large nitrate salt tanks [12], the foundation for this concept does not require active or passive cooling or insulation. This simplifies the foundation design and negates monitoring and maintenance beyond that which is standard for an industrial system. While the anticipated foundation is large, it is not expected to deviate from standard civil practice. Depending on site characteristics, a pile foundation may be appropriate.

[2] While requiring thoughtful design and economic analysis, suspending such a load is viewed as technically reasonable. Tuned mass dampers of 100's of tons have been successfully implemented atop skyscrapers. A limited market survey found commercially available spring hangers individually sized for 20 tons.

1.2.10 Ullage Gas Control System

Pressurized ullage gas is used to raise salt from the thermocline tank into the sump tank. Depending on the system design, the required gas pressure is approximately one atmosphere overpressure (i.e., 14.7 psig). When ullage the gas control system is not in operation (e.g., night or off-nominal events), the thermocline tank gas space could be depressurized to allow the salt to drain back from the sump tank and receiver into the thermocline. The system relies on gas pressure measurements to provide the feedback to gas flow controllers and actuated gas valves.

The ullage gas system could be designed to recycle the gas, or it could function as a once-through system using an in-situ nitrogen generator, compressor, and storage tank to generate and replace the daily use of ullage gas. Generators with the capacity for the envisioned systems—on the order of 0.3–3.4 Nm^3/hr (12–120 SCFH)—are commercially available. The nitrogen must be high purity, with minimal moisture and oxygen impurities, as these will readily react with the salt and impact corrosion. A once-through system may avoid many potential issues associated with handling HCl or salt vapors in the vented gas. However, the increased upfront cost of the gas generator and purifier, as well as ongoing operation and maintenance costs, must be considered. In addition, potential emissions would require evaluation and comparison to applicable regulations, and potential scrubbing. A closed ullage gas system requires a compressor and reservoir, but it avoids the costs associated with a gas generator, purifier, and emissions. However, the system must be compatible with trace amounts of HCl and salt vapors in the gas flow, in addition to longer term accumulation of such species.

1.2.11 Salt Chemistry Control

As noted in the Introduction, molten salt chemistry must be maintained to inhibit corrosion. Oxygen and water are known to lead to corrosion. Air is one potential source for oxygen and moisture. The design intentionally limits the number of potential locations for air ingression (i.e., flanges, valves, fittings, shaft seals). Trace impurities in the ullage gas and leaks in the gas system are other potential sources for oxygen. In contrast to a two-tank system, the smaller gas volumes reduce the amount of ullage gas used and the associated impurities.

Magnesium metal would be used to mitigate minor oxygen or water ingression and to maintain the salt redox potential. In the method being explored by Gen3 CSP researchers [20], magnesium would be placed in the sump tank and/or at the bottom of the thermocline tank. Both locations are on the cold side of the system. The magnesium would reduce oxides to form MgO, or it would reduce hydroxides to form MgO and HCl/H_2. Given the quiescent nature of the thermocline tank, precipitated MgO would settle to the bottom.

1.2.12 Salt Flow Control across Heat Exchanger

A control method is required for the flow of salt across the heat exchanger. As the thermocline moves axially along the tank, the differential pressure which drives the salt flow across the heat exchanger also changes. To maintain a steady cold-side salt temperature and sCO_2 exit temperature, the flow of salt needs to be regulated. During non-power cycle operations, the salt flow across the heat exchanger should be halted to maintain thermal efficiency. Two methods are conceived for flow control, a control valve, and a weir.

1.2.12.1 Control valve

The control valve concept uses a mechanical device to regulate and shut off salt flow to the heat exchanger. This valve apparatus could include several traditional valves (e.g., globe valves) placed

around the baffle. Another configuration would be to form a submerged dome over the inner region and to use a single valve to regulate flow. Other methods being considered do not use a traditional valve, but instead use a larger actuated ring that opens and closes the low path. All of these methods require actuator(s) and sealing surface(s). The control valve function is positioned in the hot section of the thermocline tank, presenting an additional challenge. Actuators likely require penetrations through the top dome of the thermocline tank. The penetrations, actuators, and sealing surfaces are all potential failure points. Maintaining a salt-compatible sealing surface is an ongoing area of research and development.

1.2.12.2 Weir

The weir concept is a simple hydraulic solution that eliminates the need for salt-wetted control valves. A weir is formed by placing perforations through the top region of the baffle. Salt is drawn into an oversized pump sump tank, lowering the salt level in the thermocline tank. As the level drops in the thermocline tank, less salt flows through the weir. To shut off the flow to the heat exchangers, the salt level is sufficiently lowered in the thermocline tank until it drops below the perforations in the baffle. This solution relies on the monitoring and control of the ullage gas space and salt level. This approach would also require the sump tank to be larger in capacity than it would otherwise need to be. While it appears to be an elegant solution, its performance during system transients must be assessed.

1.2.13 Operation Instrumentation and Control

The system requires limited data for control. The temperature of the salt that is introduced to the top and bottom of the thermocline must be controlled to maintain thermocline stability. The salt temperatures can be monitored and controlled through the following means:

1. The receiver outlet salt temperature provides feedback to adjust the speed of the salt pump via an VFD. Increasing the pump speed would decrease the outlet salt temperature, whereas decreasing the pump speed would increase the salt outlet temperature.

2. The HCHX outlet salt temperature provides feedback to a device that throttles flow into the annular region (Section 1.2.12).

3. The salt liquid level in the thermocline and sump tank is used to provide feedback to the gas control systems that regulate the ullage gas pressure in these two spaces.

In addition, the heliostats in the reflector field would also be monitored and controlled, which is standard with any CSP plant.

Based on the operation control strategy, the suite of instrumentation required to operate and monitor the system is limited, as seen in Table 2.

Table 2. Instrumentation suite

Measurement	Instrument	Comments
Liquid level	Radar level gauge	Located above the thermocline tank and sump tank; these gauges use a wave guide, and they are located away from the hot salt. These are standard commercial items. Other techniques could also be used.
Gas pressure	Pressure transducer	These transducers measure the pressure of the thermocline tank, the sump tank, and the ullage gas reservoir. These are standard commercial items.
Temperature	Thermocouples	These are standard commercial items.
Salt potential	Electrochemical sensor	These sensors are located above the thermocline tank and/or the sump tank. Some options are in development, or they are commercially available.

Note that no salt service flowmeters or salt-wetted pressure transducers are required to operate the system. The system requires only one salt-wetted flow control device (e.g., valve), as discussed in Section 1.2.12. With the quiescent tank and the type of pump used, salt filtering is also not required.

1.2.14 Solar Reflector Field

The requirements of the solar reflector field for the proposed concept are not expected to vary from the existing state-of-the-art requirements. The maturation of the concept, as with any new CSP concept, accounts for new technologies for heliostats, field layout, and O&M, for example. However, the solar reflector field design is not unique to the proposed concept.

1.2.15 sCO_2 Power Block

Commercial companies and R&D efforts are focused on development and deployment of sCO_2 power cycles (see Section 1.1). The systems under development and demonstration are sized for approximately 1–50 MW_t. For this study, the heat exchanger interface (HCHX) to the cycle and the overall thermal power of the cycles currently being pursued were considered. However, the current study remained agnostic as to the power cycle design details.

One notable tradeoff for the concept's reduced length of salt piping is the additional length of sCO_2 piping that may be required. Mitigation measures could include the following:

1. Locate the sCO_2 power cycle closer to the top of the thermocline tank. The compact size of the sCO_2 power cycle may make it may be feasible to locate smaller scale power cycles at the top of the tower, but as the system is scaled up to higher powers, this may become untenable. Additional trade-offs are associated with access for maintenance activities.

2. Include an intermediary salt loop between the top of the thermocline and the sCO_2 power cycle, as seen in Section 1.2.17.3.

1.2.16 Site Configuration and Scale-Up

There will be a practical upper limit as to the size of the thermocline tank influenced by fabrication, transportation, stability, and site-dependent foundation support. Smaller modular units can be deployed onsite to form a larger system, as in the example shown in Figure 3. Several configurations are envisioned. These could be arranged and connected for sharing or for having independent, salt sump tanks and pumps, receivers, power cycles, or tower/foundation structures. Modular units require less up-front funds, and they start generating revenue as the site, field, and/or system is expanded. Depending on the arrangement, the plant could also operate while one of the thermocline energy storage tanks is down for inspection, maintenance, or an unwanted disruption.

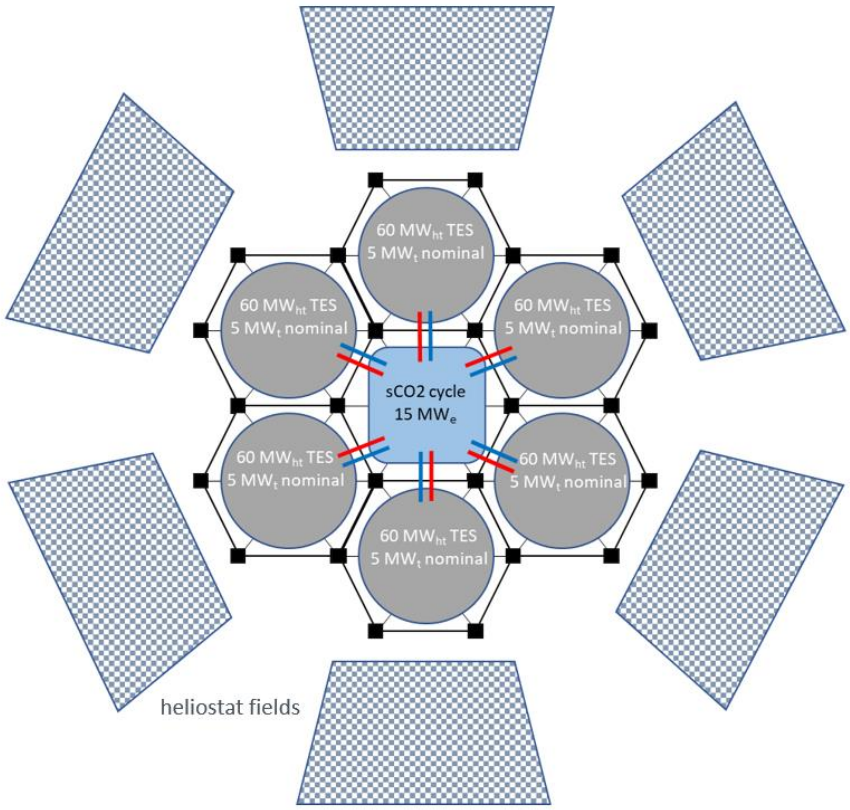

Figure 3. Example plant layout of modular units with shared power cycle.

1.2.17 Design Alternatives

1.2.17.1 System layout

Alternate system layouts are shown in Figure 4 and Figure 5.

In alternate layout 1, the riser pipe is replaced by an annular region formed by encapsulated high-temperature insulation. This arrangement removes the long insulated riser pipe, but the top head configuration has a more complex design and fabrication/installation.

In alternate layout 2, the riser pipe is external. It can use low-temperature alloys and insulation, but it would require much more external heat tracing and likely has a more complex method of differential thermal expansion accommodation (e.g., bellows).

The third alternate layout moves the hot-return pipe after the receiver to below the HCHX. This reduces the gas-space pressure required to operate the system. In this configuration, the gas space can be designed to remain below 15 psig. Keeping the design pressure of the tank below 15 psig may have advantages with respect to code compliance. The major detractor for this layout is the inclusion of a salt-wetted high-temperature penetration into the side of the vessel.

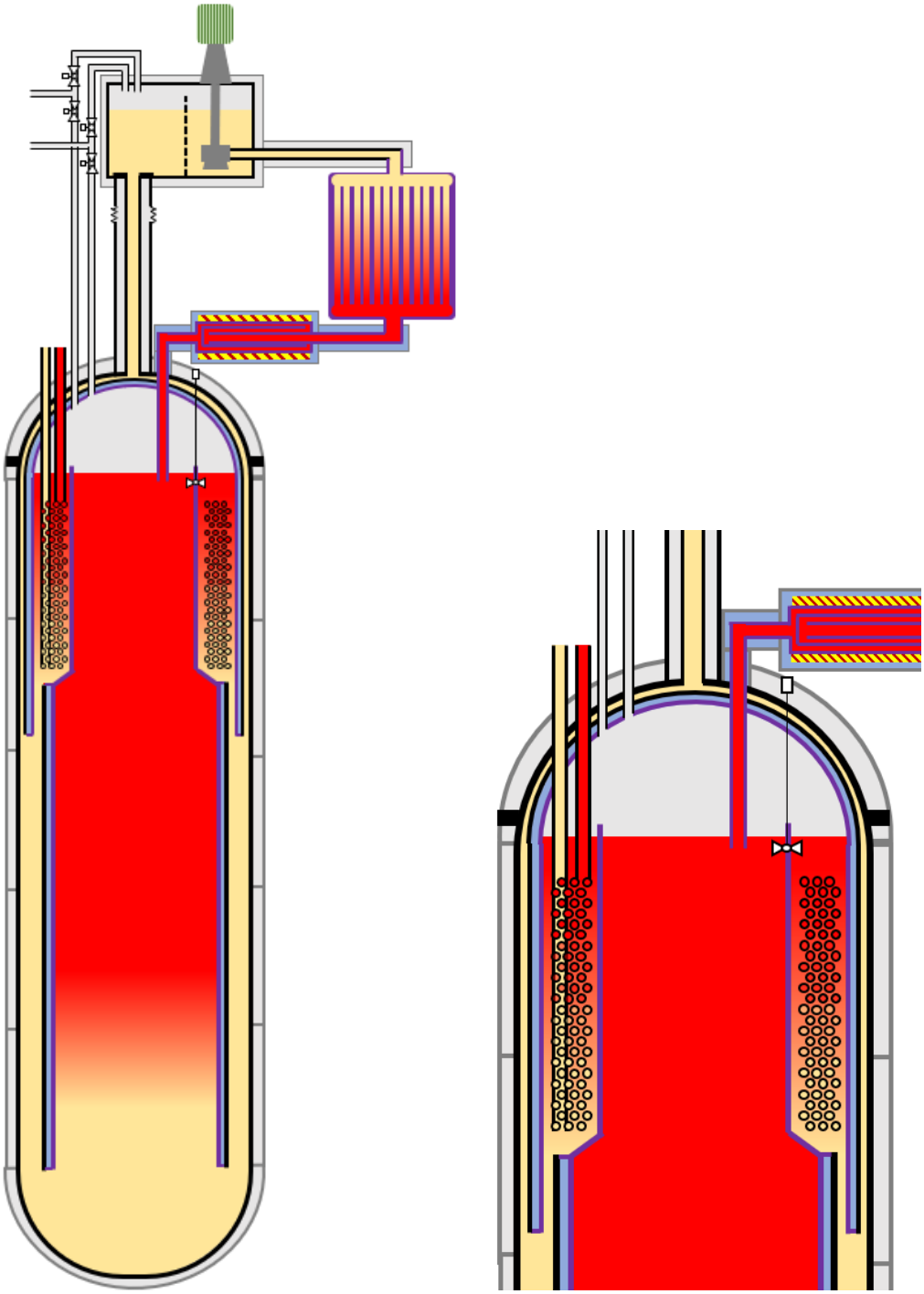

Figure 4. Alternate layout 1.

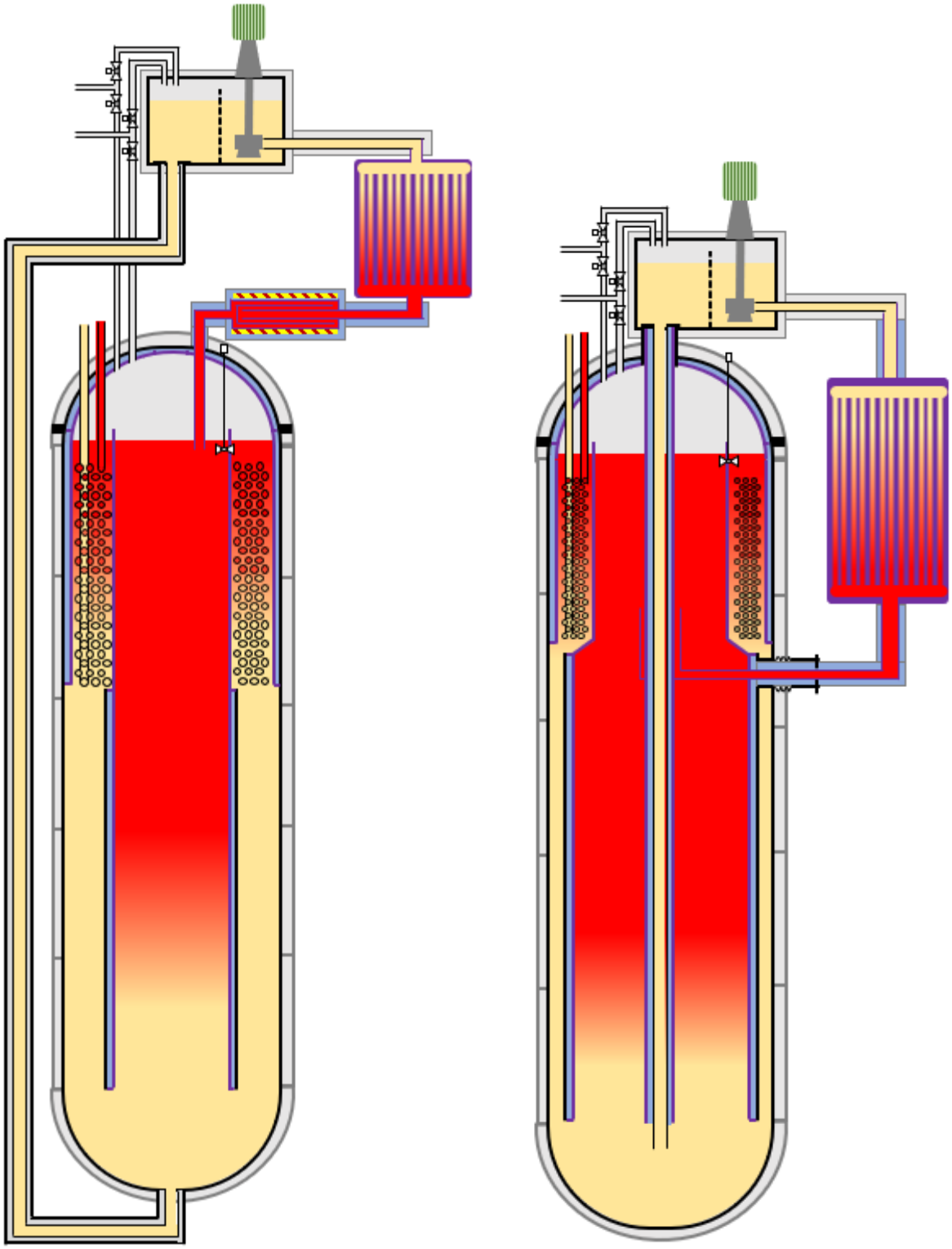

Figure 5. Alternate layouts 2 and 3.

1.2.17.2 HCHX configuration

The proposed concept uses a single large diameter HCHX. As noted in Section 1.2.1, the size limits for ground transportation can vary, depending on state regulations and the specific path. For HCHXs with diameters larger than those amenable for ground transport, options include the following:

1. Fabricate the HCHX on site or nearby. If many CSP system modules are deployed in the region, then this option may be economical.

2. Use several small HCHX units placed around the perimeter of the annular region. These could be mounted through penetrations in the top lid of the thermocline tank. This would also facilitate removal and maintenance of the HCHXs, but it would require monitoring and control of the sCO_2 through each unit and additional baffling/structures in the upper portion of the thermocline tank to direct the salt flow.

This study assumed that the HCHX was made entirely of the high-temperature alloy. Savings may result from dividing the HCHX into high- and low-temperature sections. The low-temperature section could be constructed of a lower cost material. The challenge with this approach is to ensure that the low-temperature section is not exposed to the high temperatures, such as during off-nominal events. Operational experience would inform whether this approach is reasonable.

1.2.17.3 Intermediate salt loop

An intermediate salt loop could be added between the TES tank and the power cycle. This would decrease the amount of thick-walled piping required for the high-temperature and high-pressure sCO_2. This would also provide an intermediate system to mitigate any sCO_2-to-salt leaks. However, an intermediate loop would increase costs for additional components (e.g., pump, heat exchanger, instrumentation) and associated O&M costs, and the loop could increase technical risk (e.g., pump failure, heat exchanger fouling).

1.2.17.4 Flanged vs. welded tank construction

As noted above, tank segments can either be welded or flanged together. Flanges require additional material, seals, and bolting. Beyond additional weight and cost, flanges are also potential leakage/failure points. An all-welded tank with a single flange located in the top gas space was selected for the preconceptual design to allow for replacement of the HCHX. It is likely advantageous to remove this flange for N^{th}-of-a-kind systems.

1.2.17.5 Alternate power cycles

Other power cycles that could be used in lieu of the sCO_2 cycle could be driven by the proposed concept. Ultra-supercritical steam power cycles are currently adopted by the power industry, and the technology continues to advance. These power cycles approach operating temperatures that align with the proposed chloride-salt concept, but they operate at pressures considerably higher than those of the sCO_2 cycle. Another alternative would be to use an open-air Brayton cycle. The heat addition from the chloride salt concept is at the lower end of temperatures for cases in which this technology is typically operated. An advantage of the open-air Brayton cycle, especially for arid regions, is the reduction and/or elimination of the cooling system as part of the power cycle. Whereas the open-air Brayton cycle is a mature technology in the natural gas power and jet engine industries, coupling and demonstrating the technology with a molten salt system would require development effort.

1.3 SUMMARY COMPARISON TO EXISTING PLANTS

The proposed concept has several advantages over a traditional two-tank system, as discussed in Sections 1.2.1 through 1.2.16. Key advantages to include:

- Unique thermocline tank design enhances economics.
  - One salt tank is required instead of two.
  - Most of the thermocline tank is in contact with cold salt, which facilitates the use of less expensive structural materials.
  - The tank support concept readily accommodates tank thermal expansion and negates the complications of foundation thermal management.
  - Co-locating the single tall tank within the tower results in more area being available around the tower for the solar reflector field.
  - Using a modularly constructed tank that is fabricated at a factory reduces the amount of onsite construction needed.
  - Less ullage gas is required.
  - No filler material is included, thus eliminating the thermal ratcheting phenomenon.

- Substantially less components are required, thus reducing hardware and O&M costs.
  - One short-shafted cold-salt pump is required instead of one cold-salt and two typically long-shafted hot-salt pumps. No high-head pumps are needed. Unlike long-shafted pumps, short-shafted pumps do not require salt-contacted bearings, have been employed for high-temperature salt service, and are more readily removed for maintenance.
  - Either one or no salt-wetted valves are required in contrast to >10 typically used in traditional plants.
  - Substantially less hot- and cold-salt piping is required, thus reducing the number of piping connections and the trace heating and insulation requirements.

- There are some technical challenges compared to traditional two-tank system.
  - The baffle likely requires high-performance (i.e., more costly) insulation.
  - Thermocline stability requires further research and thoughtful system operation.

2. CHLORIDE SALT SYSTEM POINT DESIGNS

This section presents the analysis method and the results obtained for concept point designs for a range of scales. The analysis was performed to generate rough estimates for system size and mass to be used with for different scale systems. It must be stressed that these point designs were not optimized for performance or economic, and as discussed in Section 2.1, more rigorous design and analysis methods may be performed in the future.

2.1 0-D DESIGN AND ANALYSIS METHODS

2.1.1 Applicable Standards

The ASME BPVC VIII-1 applies to fired or unfired vessels operating at pressures higher than 15 psig. The code covers design methods, construction, and fabrication techniques. BPVC Section II provides allowed stress values as a function of temperature for a wide range of materials (i.e., standard compositions, forms, and specifications) used in VIII-1 and other vessels. The ASME B31 code covers requirements for power piping (B31.1) and processing piping (B31.3). Both the BPVC and B31 codes cover applicable design and fabrication details for the envisioned system.

The American Petroleum Institute (API) 620 and 650 standards are applicable for the vertical above-ground storage tanks typically used in the petrochemical industry. Although API 620 extends up to 15 psig (0.2 MPa), both codes are constrained to low temperature operation (e.g., up to 250°F [121°C] as specified in API 620). However, some practices and intents may apply to the envisioned system.

2.1.2 Material Properties

The assumed salt properties are summarized in Table 3. A constant value for specific heat was used in the scoping design because it is a weak function of temperature. The temperature-dependent properties for supercritical carbon dioxide [27] are assumed at an operating pressure of 25 MPa.

Table 3. Assumed salt properties for sizing analysis

Property	**NaCl-KCl-$MgCl_2$ [20]**	**Solar salt (60% $NaNO_3$, 40% KNO_3) [26]**
Density (kg/m^3)	$1974 - 0.5878 \times T_C$	$2090 - 0.636 \times T_C$
Viscosity (Pa s)	$(6.89 \times 10^{-4}) \times EXP(1224.73/ T_K)$	$0.022714 - 0.120 \times 10^{-3} \times T_C + 2.281 \times 10^{-7} \times T_C^2 - 1.474 \times 10^{-10} \times T_C^3$
Thermal conductivity (W/m K)	$(7.151 \times 10^{-7}) \times T_C^2 - (1.066 \times 10^{-3}) \times T_C + 0.811$	$0.443 + (1.9 \times 10^{-4}) \times T_C$
Specific heat (J/kg K)	1,011 (at 625°C)	1,538 (at 550°C)

*where T_K is the temperature in units of Kelvin, and T_c is the temperature in units of Celsius

When estimating masses, the densities were assumed to be those listed in Table 4. The allowed temperature-dependent stresses that were used for the metals are from the 2019 ASME BPVC. Values for plate-type product forms were used to determine wall thicknesses. The design temperature for the cold alloy was assumed to be 25°C higher than the planned cold-side operating temperatures. The design temperature for the hot alloy is assumed to be 10°C higher than the planned hot-side operating

temperatures. Values for bolting were used to size the flange head bolting. Although factors such as material specifications, heat treatment, and code application specifics influence the allowed stresses for real systems, the current approach is deemed sufficient for the purposes of a preconceptual design.

2.1.3 Weighted Cost Metric and Value Metric

The mass of the various materials required for the preconceptual design was calculated. The total system mass was one metric for design studies and optimization, but because there are substantial cost differences between materials (e.g., salt vs. nickel alloys), a weighted cost metric was used when comparing designs. The weighted cost metric is the summation of the individual material costs using the pricing assigned per Table 4. The scope of materials included are as follows: thermocline tank, baffle, riser pipe, sump tank, receiver, piping to the receiver, receiver tubes and top and bottom headers, return piping and thermal muffler after the receiver, HCHX, and insulation associated with these components. Major components such as the supporting superstructure, foundation, salt pump, receiver enclosure, reflector field, and power cycle were not included in the cost estimation. Furthermore, additional costs are associated with components, fabrication, transportation, field installation, financing, infrastructure, operation, and maintenance that are not captured in this study. The predicted cost was used as a weighted metric to provide insight into tradeoffs in sizing the preconceptual design: it is not intended to reflect the cost of an actual system.

Table 4. Assumed material density and prices for cost metric

Material	Density	Assigned cost	
	kg/m^3	$/kg	$/lb
Hot alloy plate/sheet	8,360	44.00	20.00
Hot alloy tube/pipe	8,360	88.00	40.00
Cold alloy plate/sheet	7,990	6.60	3.00
Cold alloy tube/pipe	7,990	13.20	6.00
Outside insulation	128	3.33	1.51
Inside insulation	430	17.08	7.76
Salt	*See Table 3*	0.35	0.16
Mg	-	2.5	1.14

A value metric was defined by the ratio of the weighted cost metric to the net power produced ($/kW$_{t\text{-}h\text{-}day,\ net}$). The net power produced is the nominal power generated per day reduced by the predicted thermal losses. Other energy sources and sinks (e.g., pump power, instrumentation, insolation on the system other than the receiver, trace heating) were not considered in the net power.

2.1.4 Thermocline Vessel Shell, Top Head, and Bottom Head

The required shell thickness, *t*, was determined using the Eq. (1).

$$t = P \times R / (S \times E - 0.6 \times P + \text{corrosion} + \text{tolerance}, \quad (1)$$

where *P* is the maximum allowed working pressure, *R* is the radius, *S* is the maximum allowed stress, and *E* represents weld efficiencies.

The weld efficiencies, *E*, were prescribed. For the cold alloy material forming the outer pressure boundary, a weld joint efficiency of 0.85 was assumed. In practice, this value can be increased to 1.0 with extensive post-weld inspection such as radiography. For the preconceptual design, less extensive inspection of the large tank sections was assumed. Ultimately, the choice and extent of weld inspection would be based on code requirements and techno-economic analysis. For the hot metal material, a weld efficiency of 1.0 was assumed. Given the high cost of the material, it was assumed that the more extensive weld analysis would be favored in a technoeconomic optimization.

The radius, *R*, was taken as the tank's OD.

The maximum allowed working pressure, *P*, for the shell and the top and bottom heads was determined by the maximum gas space pressure in the pump sump tank (i.e., specified) and the hydrostatic pressure of the salt at the location of interest. The hydrostatic pressure is based on the cold-salt density (i.e., conservative) and the calculated heights for the design. Note that the hydrostatic pressure in the bottom of the tank is significant given the height of the vessel. Only internal pressurization was considered in the sizing (i.e., vacuum conditions were not calculated). Vacuum conditions will require analysis in the future.

The corrosion allowance for all hot and cold alloy materials was specified assuming 30 μm/y for 30 years (i.e., 0.9 mm [0.035 in.]).

A tolerance of 0.254 mm (0.010 in.) was added to the required thickness to account for plate material tolerances. Finally, a minimum thickness of 3.175 mm (0.125 in.) was set to prevent unreasonably thin walls for such a system.

Two configurations were considered for the shell. The first configuration is a uniform thickness shell based on the required thickness for the bottom of the shell (i.e., highest hydrostatic pressure). For the second configuration, the required wall thickness was determined at various axial positions along the shell (i.e., customized wall thicknesses reflecting the reduction in hydrostatic pressure along the length of the vessel).

Finally, it should be noted that other potential stresses on the vessel, such as dynamic loads caused by wind or seismic effects, were not considered.

The heads of the tank were assumed to be ellipsoidal, with the diameter being four times larger than the height. The required top and bottom head thicknesses were calculated to be similar to the shell thickness using Eq (2). The *K* factor is 0.9 for the ellipsoidal head geometry assumed.

$$t = P \times D \times K / (2 \times S \times E - 0.2 \times P) + \text{corrosion} + \text{tolerance}, \quad (2)$$

where *D* is the shell outer diameter and *K* is a head geometry factor.

2.1.5 Vessel Insulation and Heat Loss

The thickness of the insulation surrounding the vessel and the material (mineral wool or Pyrogel) is specified. The ambient temperature and convection coefficient are also specified. The temperature of the insulation's inner surface is assumed to be equal to the cold-salt temperature.

The heat loss through the wall to the ambient environment was then determined, accounting for the thermal resistance of the insulation and convection on the exterior. The temperature-dependent thermal conductivity of the insulation was accounted for by numerically discretizing the insulation into ten regions. The thermal resistance of the vessel wall was negligible compared to the insulation and was not included in calculation.

A nominal ambient temperature of 21.1°C (70°F) and a convective coefficient of 50 W/m K were assumed. Additional calculations were performed to investigate the surface temperature and heat losses under the extreme conditions of 46.1 and 0°C.

2.1.6 Baffle

It is desirable to balance the flow of heat into and out of the annular region. Therefore, the thickness of insulation in the baffle should be determined based on matching the heat flow through the baffle with the heat loss to the environment.

Various possible configurations of the baffle were considered. The high-performance microporous insulation was down-selected to limit the thickness of the baffle, thereby decreasing overall system dimensions. Traditional refractory insulating bricks or fiber insulation was found to result in relatively thick baffles (e.g., >25 cm). To house the microporous insulation, the baffle was assumed to be constructed with an inner layer of high-temperature metal and an outer wall of low-temperature metal.

The baffle is not a pressure boundary with respect to system integrity and safety. Materials that are not code qualified could be used, but the choice of materials and the allowed stresses were constrained to those considered for the vessel wall. Furthermore, a single plate thickness was used for all regions of the baffle to simplify sourcing. It may be possible to use thinner material for the upper regions of the baffle than that used for the lower regions of the baffle.

For the proposed baffle configuration, the annular space is pre-pressurized with gas to resist the system's hydrostatic pressure. The baffle is sealed at ambient temperature during fabrication, so it pressurizes when the system is heated during operation. The required initial pressure at the ambient temperature of a baffle segment is determined using Eq. (3):

$$P_a = P_{hyd} \frac{T_a}{\frac{(T_c+T_h)}{2}}, \tag{3}$$

where

P_a is the required initial baffle pressure during fabrication at T_a,
P_{hyd} is the system hydrostatic pressure at the bottom elevation of baffle segment during operation,
T_a is the ambient temperature, which is assumed to be 25°C (298 K),
T_h is the specified hot-side salt temperature in Kelvin, and
T_c is the specified cold-side salt temperature in Kelvin.

The required outer wall thickness of the baffle, which is based on a simple thin-walled cylindrical shell, must meet two conditions:

1. It must resist a specified differential pressure of 103.4 kPa (15 psi) at the hot-salt temperature.
2. It must resist the initial pressurization of *Pa* at ambient temperature.

Therefore, the required metal shell thickness is the greater of these two conditions, along with the hot-material corrosion allowance and an additional 0.25 mm (0.01 in.) to account for plate tolerances. Finally, the minimum wall thickness was constrained to 1.59 mm (1/16 in.) to prevent impractical wall thickness for this type of an engineered system. A buckling analysis of the cylindrical baffle sections was not considered and is noted as another factor for future design refinement.

2.1.7 HCHX

The HCHX is assumed to be a triangular-pitch tube bundle in crossflow. Cold sCO_2 enters the bottom of the HCHX tubes and exits from the top manifold. Hot salt passes downward across the outside of the tubes. In this configuration, the HCHX operates in counterflow. Furthermore, a once-through design was chosen for the tube-side sCO_2 and the shell-side salt.

For baseline geometry, the tubing has an OD of 19.1 mm (0.75 in.). The sCO_2 outlet velocity was fixed at 10 m/s. The desired sCO_2 inlet and outlet temperatures were also specified. With target total power, exit velocity, tube geometry, inlet and outlet temperatures, and sCO_2 thermophysical properties, the total number of required tubes can be determined. For the baseline geometry, 239 tubes are required. There are 8 tubes across the width of the HCHX that sits within the annular gap. The tubes' center-to-center distance is 1.25× the OD of the tubes. The height of the HCHX is 3.81 meters. Based on the desired minimum and maximum salt temperatures, the salt thermophysical properties, and the desired power output, the required mass flow rate of the salt through the HCHX can be determined.

The total salt flow rate across the heat exchanger is calculated based on the desired salt differential temperature, heat removal, and specific heat. For the baseline design, this is 24.73 kg/s:

$$m_{flow}=C_p \times (T_h - T_c). \quad (4)$$

where, C_p is the salt specific heat, T_h is the hot salt temperature, and T_c is the cold salt temperature.

Equations for temperatures and heat transfer were developed and solved iteratively. The HCHX was discretized into 10 regions axially. Conservation of energy was applied to each axial region for both the salt and sCO_2 sides. For each axial region, average salt and sCO_2 temperatures were determined. Using their average temperatures, system geometry and flow rates, the salt and sCO_2 properties, velocities, and Reynolds number were evaluated. An engineering correlation for crossflow tube bundle heat transfer [28] was used to determine a convective heat transfer coefficient for the salt side. Similarly, an engineering correlation (Dittus-Boelter) was used to determine the heat transfer coefficient for the sCO_2 side. With these heat transfer coefficients and the thermal resistance across the tube wall, an overall heat transfer coefficient for each axial level was determined. Coupled with the average axial level temperatures, the overall heat transfer coefficient was used to determine the heat transfer from the salt to the sCO_2 at each axial level. Finally, the total heat transfer across the HCHX was calculated through summation of the heat transfer at each of the 10 axial levels. As noted, this set of equations was solved iteratively. With the baseline geometry specified, the overall height of the heat exchanger was varied until the desired power was reached.

In a manner similar to determination of heat transfer, the salt side and sCO_2 side pressure drops were determined at each axial level. The overall pressure drops were determined by summing the 10 axial levels.

2.1.8 Sump Tank

The top and bottom of the sump tank were assumed to be ellipsoidal heads like the thermocline tank. The diameter of the tank was assumed to be half the diameter of the thermocline tank. The depth of the salt in the tank is specified (0.60 m assumed for base case). The thickness of the walls for the sump tank were determined using the methods described in Section 222.1.4 for the thermocline tank.

Metal baffles would likely be included in the sump tank to inhibit sloshing and gas entrainment, but their sizing and distribution have not been evaluated.

2.1.9 Vessel Flange

Two half-flanges (i.e., top dome) were included in the design, with the flange located above the salt-free surface (i.e., 0.5 m in the baseline design).

A gasket load of 2,750 lb/in. was assumed to be required for sealing. This load represents metal ring gaskets such as those used in aerospace applications (high temperature) and nuclear reactor pressure vessels (large diameter). The total required bolt load was determined based on the summation of the gasket load and the gas space pressure.

The spacing between bolts (i.e., center-to-center) was assumed to be 4× the bolt diameter. Based on this spacing and the vessel's diameter, the maximum number of bolts was determined for different bolt sizes. The allowed stress for the bolt material (i.e., 316, SA-193 B8M S31600 Class 1 for the base design) was then used to determine to the total load the bolts can handle for a give bolt size. Finally, the needed bolt size and number was determined by comparing the allowed load with the required load.

With the number and size of bolts determined, a simplified approach was used to size the flange. The width of the flange (i.e., in the radial direction) was assumed to be 3× the bolt diameter. The total thickness of the assembled flange was 2.5× the bolt diameter (i.e., 1.25× thickness for each of the mating faces).

2.1.10 Design Criteria and Constraints for point designs

Several additional design criteria were specified for the preconceptual designs:

a. Outside vessel surface less than 60°C (140°F)

b. Meets power and TES capacity goals (1–50 MW_t with 12 hr of storage [i.e., 12–600 MW_{ht}])

c. Tank wall thickness satisfies material-allowed stresses according to ASME methodology or API / American Water Works Association (AWWA)

d. TES max temperature of at least 725°C (chloride) and 565°C (nitrate salt)

e. TES min temperature of at least 500°C (chloride) and 260°C (nitrate salt)

f. Peak stainless-steel wall temperature of less than 600°C (chloride salt)

2.2 EXAMPLE DESIGN SCOPING RESULTS

Several different point designs for systems with different capacities were developed based on the simple model described in Section 2.1.

In addition to the boundary conditions and constraints discussed in Section 2.1, the following conditions were applied unless otherwise stated:

- The insulation around the tank was specified to be 400 mm (15.75 in.). For heat loss calculations, the ambient temperature was specified to be 21.1°C (70°F) with a 50 W/m K outside convection coefficient. These conditions resulted in approximately a heat loss of 100 W/m^2 from the thermocline tank.

- The hot- and cold-wall corrosion allowances were set to 0.9 mm based on 30 μm/y for 30 years.

- The tubing arrangement of the HCHX was held constant with 19.1 mm OD tubes and 8 tubes spanning a 261.2 mm annular gap space.

- The hot salt temperature was set to 725°C, and the cold salt temperature was set to 525°C.

- The sCO_2 outlet and salt inlet temperature to the HCHX were held constant and were specified to be 700 and 725°C, respectively. The sCO_2 inlet temperature was set to 500°C. The sCO_2 exit velocity within the tube bundles was set to 10 m/s.

- The receiver tubes were 9.53 mm OD (0.375 in). The target inlet Reynolds number for each receiver tube was set to 5,000. A uniform net heat flux from the receiver tubes to the salt was set to 600 kW_t/m^2. A temperature-independent design limit for the receiver tube wall was set to 12.3 MPa. A specified salt velocity of 1 m/s was used to size the inlet and return piping from the receiver.

- The salt level in the sump tank was assumed to be 0.60 m.

- The salt level in the thermocline tank was assumed to be 0.50 m below the shell-head flange and 0.25 m above the HCHX entrance

- All systems were sized for a 12-hr TES capacity at nominal power. The receiver was sized to support simultaneous charging of the TES over 8 hr while also providing the nominal power to the power cycle. For example, over the course of a day, a 5 MW_t system could provide 100 $MW_{t\text{-}h}$ to the power cycle, including 40 $MW_{t\text{-}h}$ during the day (while charging) and 60 $MW_{t\text{-}h}$ through discharging the TES.

- The thermocline tank length-to-diameter ratio was held constant at 8.

All cases met the key design criteria. Although it is not given in the table, the maximum stainless-steel vessel temperature was 525°C.

Table 5. Summary of nonoptimized systems

System size	Nominal discharge power	MWt	**1**	**5**	**10**	**15**	**20**	**25**
	Energy storage capacity	MWt-h	**12**	**60**	**120**	**180**	**240**	**300**
	Nominal power/day	MWt-h/day	**20**	**100**	**200**	**300**	**400**	**500**
	Receiver capacity	MWt	2.5	12.5	25	37.5	50	62.5
	Total system height	m	27.9	45.9	57.1	65.1	71.4	76.9
Tank detail	Tank height	m	26.6	44.5	55.6	63.5	69.8	75.2
	Shell outer diameter	m	3.1	5.2	6.5	7.4	8.2	8.8
	Shell thickness (max)	mm	8.4	21.3	32.7	42.1	50.8	58.8
	Bottom head thickness	mm	6.5	17.2	26.6	34.3	41.5	48.0
	Top head thickness	mm	3.2	3.2	3.2	4.0	4.7	5.4
	Outside heat loss	MWt-h/day	0.6	1.8	2.8	3.6	4.4	5.1
	Outside insulation surface temp.	°C	23.1	23.1	23.1	23.1	23.1	23.1
	Flange outer diameter	m	3.4	5.5	6.9	7.8	8.6	9.2
	Bolt size	mm	44.5	50.8	57.2	57.2	63.5	69.9
	Number of bolts	-	56	81	90	92	102	100
	Overpressure req.	psig	9.7	13.8	16.3	18.1	19.5	20.8
Riser pipe	Riser pipe inner diameter	mm	77.7	156.4	211.5	252.4	286.2	315.7
	Riser pipe total length	m	26.3	43.7	54.5	62.1	68.2	73.5
Baffle	Baffle outer diameter	m	3.0	5.07	6.4	7.2	8.0	8.6
	Inner wall thickness	mm	3.8	5.6	6.8	7.5	8.2	8.7
	Insulation thickness	mm	95.3	98.4	98.4	98.4	98.4	98.4
	Outer wall thickness	mm	2.9	5.9	8.6	10.7	12.8	14.6
	Thermocline velocity	mm/s	0.52	0.86	1.08	1.24	1.35	1.46
Receiver	Total height	m	3.1	3.1	3.1	3.1	3.1	3.1
	Panel width	m	1.4	6.8	13.5	20.3	27.1	33.9
	Tube inner diameter	mm	6.9	6.9	6.9	6.9	6.9	6.9
	Tube thickness	mm	1.3	1.3	1.3	1.3	1.3	1.3
	Number of tubes	-	142	711	1,422	2,134	2,845	3,556
	Thermal muffler length	m	0.85	1.39	1.72	1.95	2.15	2.31
HCHX	Tube outer diameter	mm	19.05	19.05	19.05	19.05	19.05	19.05
	Tube wall thickness	mm	5.00	5.00	5.00	5.00	5.00	5.00
	Heat exchanger height	m	1.64	3.81	4.95	5.84	6.56	7.19
	Tube pitch	mm	27.50	27.50	27.50	27.50	27.50	27.50
	Number of tubes	-	48	239	478	718	957	1,196
	sCO_2 pressure drop	MPa	0.97	0.74	0.60	0.54	0.50	0.47
	Salt flow rate	kg/s	4.9	24.7	49.5	74.2	98.9	123.6
	Salt inlet temperature	°C	725	725	725	725	725	725
	Salt outlet temperature	°C	535	524	525	525	525	525
	sCO_2 flow rate	kg/s	4.0	19.8	39.5	59.3	79.1	98.8
	sCO_2 exit velocity	m/s	10.0	10.0	10.0	10.0	10.0	10.0
	sCO_2 inlet temperature	°C	510	499	500	500	500	500
	sCO_2 outlet temperature	°C	700	700	700	700	700	700
Mass sum.	High T metal mass	tonne	19.8	83.7	148.0	208.2	267.2	324.0
	Low T metal mass	tonne	24.2	154.2	361.9	601.6	871.4	1,164.7
	Salt mass	tonne	319.0	1,494.9	2,917.8	4,331.5	5,739.1	7,141.6
	Outside insulation mass	tonne	16.1	42.3	64.9	83.8	100.6	116.1
	Inside insulation mass	tonne	10.9	32.7	52.1	68.6	83.6	97.6
	Total suspended mass	tonne	387.0	1,797.6	3,526.6	5,268.3	7,029.0	8,803.6
	Weighted cost metric	$	1.77E+06	7.53E+06	1.37E+07	1.97E+07	2.58E+07	3.19E+07
	Value metric nominal	$/kWt-h	88.4	75.3	68.5	65.7	64.5	63.7
	Value metric weight loss	$/kWt_net -h	91.3	76.6	69.4	66.5	65.2	64.4

The mass of the thermocline tank (i.e., salt, vessel, insulation) is shown in Figure 6. Results for two different thermocline tank length-to-diameter ratios are shown. There is a nearly linear increase in system mass with nominal power. The major contributor to weight is the salt mass (i.e., 78–83% across all cases). There are minor gains in reducing the thermocline tank length-to-diameter ratio.

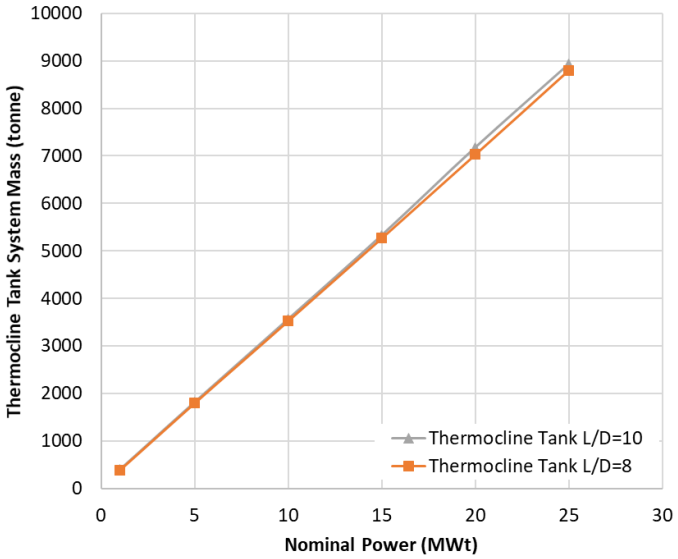

Figure 6. Variation of thermocline tank weight for various point designs.

The weighted cost metric (see Section 2.1.3) is shown in Figure 7. Similar to the increase in mass, the weighted cost metric increases nearly linearly with system size.

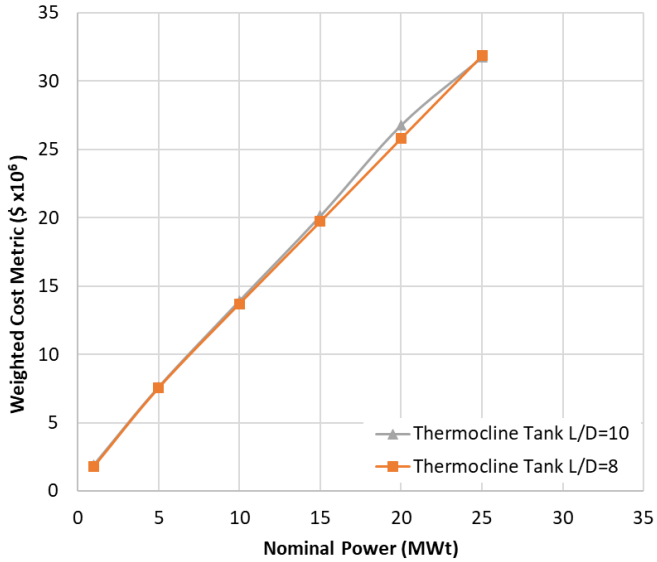

Figure 7. Variation in weighted cost metric for various point designs.

The value metric (see Section 2.1.3) accounting for thermal losses is shown in Figure 8. There is a clear improvement in the value metric going from 1 to 5 MW_t. Beyond the 5 MW_t system, there is continued gradual improvement. Included in the figure is an additional series where the sCO_2 heat exchanger was sized to have a constant sCO_2 pressure drop of 1 MPa in contrast to having a fixed sCO_2 outlet velocity of 10 m/s. As shown, the different heat exchanger constraint had a minor impact on the value metric.

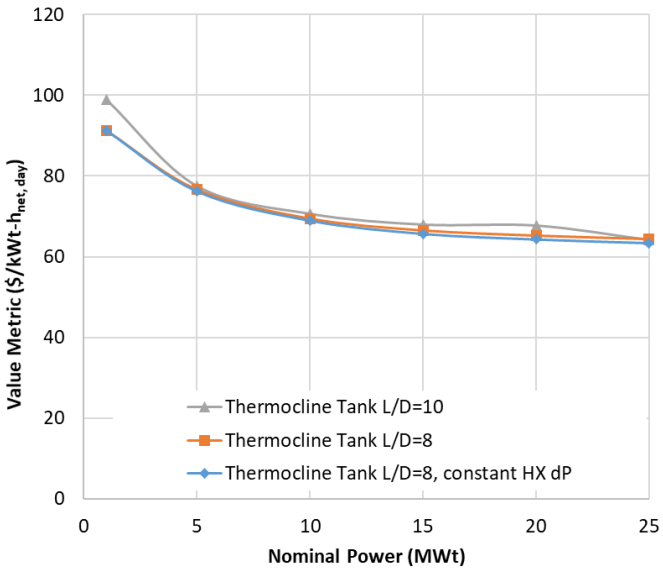

Figure 8. Variation in value metric for various point designs.

2.2.1 Additional Sensitivities for 5 MW_t System

2.2.1.1 Thermocline tank L/D ratio

The thermocline tank's length-to-OD ratio (L/D) was varied from 6 to 12. The value metric was relatively insensitive to the variation, as shown in Figure 9. The impact of the prescribed tank ratio on the tank, baffle, and HCHX OD and tank length are provided in Figure 10. As discussed in Section 1.2, ground shipments would be limited by height, width, and length constraints. With the tank's complex design, it is desirable to be able to transport the HCHX as a single unit. The range of diameters listed are all large. As the length of the tank increases, the required gas overpressure in the top of the thermocline increases. There may be considerable cost savings associated with keeping the system pressure design and rating below the mystical 15.0 psig discriminator for vessel code requirements.

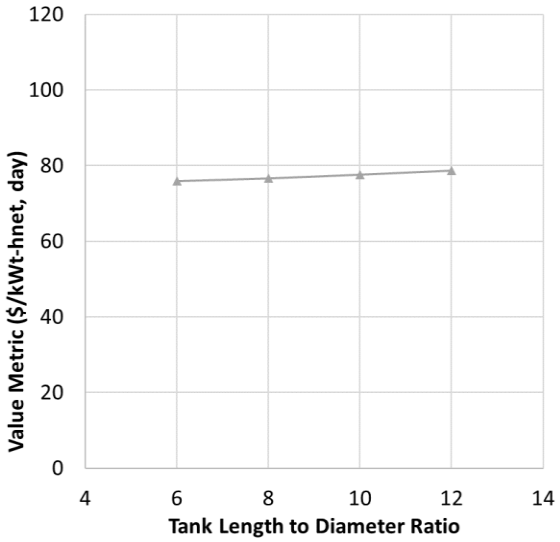

Figure 9. Variation in value metric–to–tank L/D ratio.

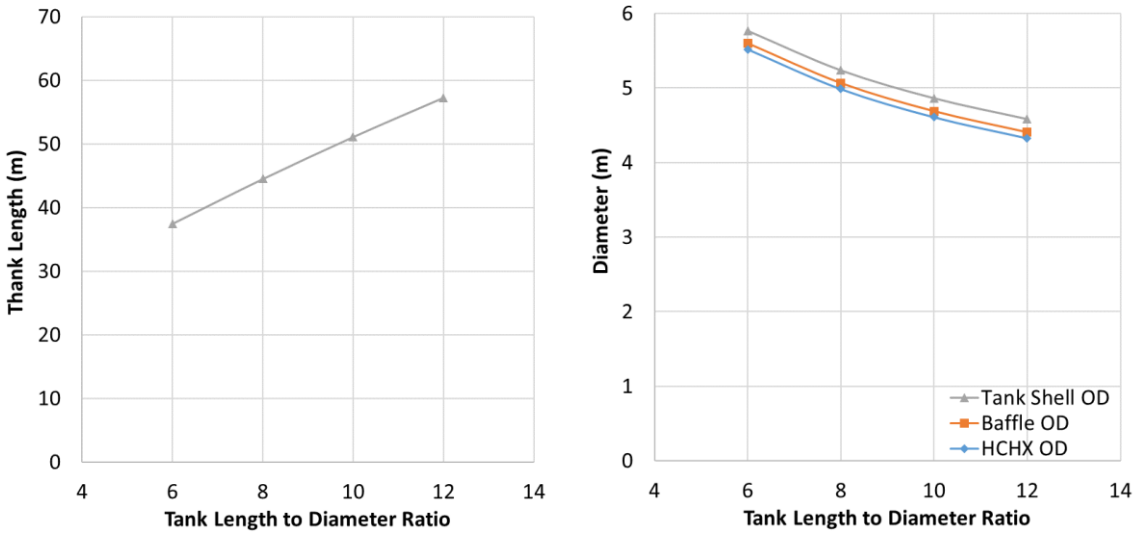

Figure 10. Variation on system dimensions with tank L/D ratio.

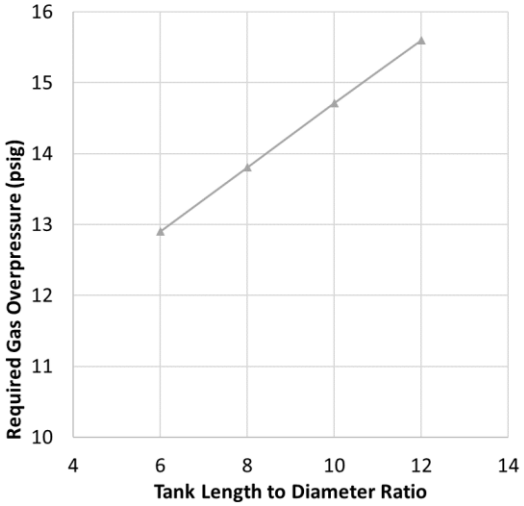

Figure 11. Required system gas pressure for various tank L/D ratios.

2.2.1.2 Insulation thickness

The outside insulation thickness was varied. Reducing the outside insulation thickness yields an expected thermal loss increase, decreased system thermal efficiency, and decreased cost. As discussed in Section 2.1.6, the baffle insulation thickness is adjusted to balance the heat transfer from the salt in the inner area of the tank to the outer annulus with the heat loss from the outer annulus to the environment. Therefore, a reduction in the outside insulation thickness leads to a proportional reduction in the inside insulation's thickness. The baffle displaces salt that could otherwise be used for TES. Therefore, with a fixed TES capacity, a reduction in baffle thickness results in an overall smaller system (tank length and diameter). Taken together, these effects result in an improved weighted cost metric when the outer insulation thickness is reduced. Also, despite the higher thermal losses, the value metric is reduced (i.e., improved) by decreasing the outer insulation thickness, as shown in Figure 12.

However, the model does not capture the complex conduction and convection of heat across the annulus. Heat transfer into and out of the annulus would cause convection cells to form within the annulus. The temperature difference driving the convection cells increases with the magnitude of the heat being transferred. The convection cells would encourage axial temperature variations within the annulus and baffle. Ultimately, these variations can influence the stability of the thermocline. A computational fluid dynamics simulation of the annular region could quantify the effect of these convection cells.

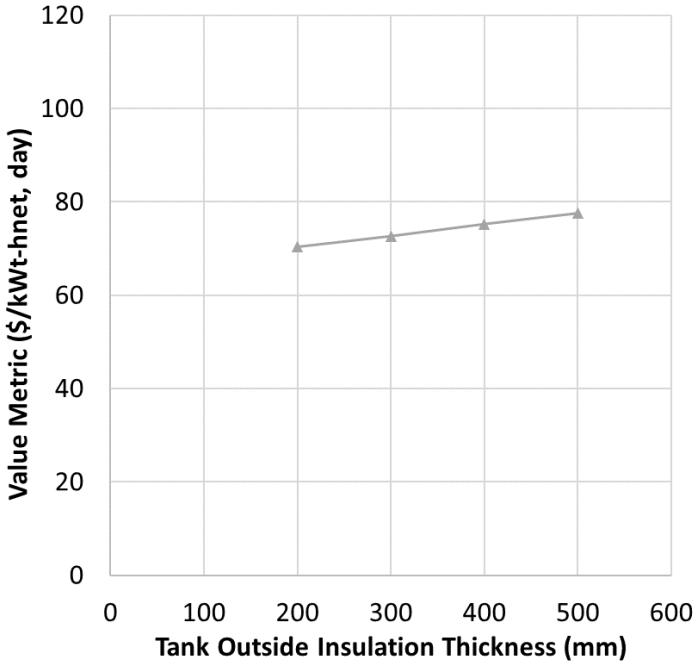

Figure 12. Value metric vs. outer insulation thickness.

2.2.1.3 HCHX design

The number of tubes across the width of the HCHX was varied between 6–10, and the OD of the tubes was varied between 12.7 and 25.4 mm (0.5–1.0 in.).

Increasing the number of tubes across the width of the HCHX effectively decreases the velocity of the salt through the heat exchanger. The reduced velocity degrades the salt-side heat transfer coefficient. A larger HCHX (tube surface area) is needed to offset the poorer heat transfer. Ultimately, increasing the number of tubes across the width of the HCHX results in an increase in the value metric.

Increasing the diameter of the tubes while keeping the outlet velocity fixed reduces the number of HCHX tubes required. However, with the increase in diameter, the tube wall thickness increases. Also, with a tube center-to-center spacing of 1.25× the tube diameter and the number of tubes across the HCHX being fixed (i.e., 8), the increase in tube diameter results in more flow area for the salt side. The increased flow area results in lower salt velocities, lower heat transfer coefficients, and the need for a larger surface area. Ultimately, more HCHX tube mass is required as the tube diameters increase.

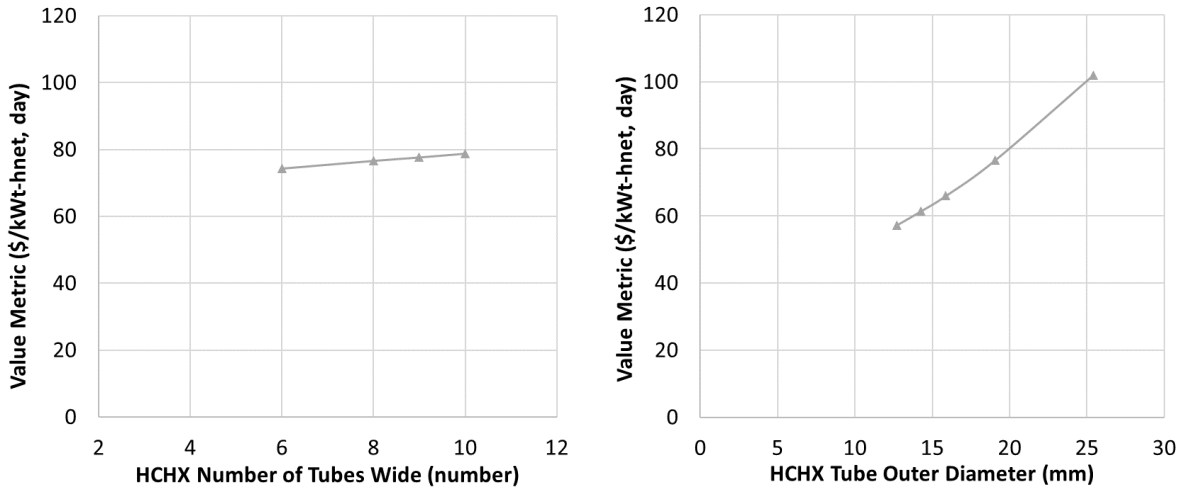

Figure 13. Variation of HCHX tube bundle.

It should be noted that the weighted cost and value metrics are based on the weighted cost of material based on mass. The costs related to fabrication details, such as the number and type of welds and weld inspections, are not captured. As noted earlier, as the diameter of the tubes increases, less tubes are needed (based on the applied constraint that the sCO_2 outlet velocity remain 10 m/s). Conversely, when the diameter is decreased, the wall thickness decreases, more parallel tubes are needed, and the value metric decreases.

2.2.1.4 System temperatures

The maximum salt and sCO_2 temperatures were varied. The results for varying each parameter independently and together are illustrated in Figure 14. For all cases, the cold-salt temperature of 525°C, and the sCO_2 inlet temperature of 500°C were held constant. Note that for the baseline case, there is a difference of 25°C across the HCHX at the top (hot salt inlet and hot sCO_2 outlet) and bottom (cold salt outlet and cold sCO_2 inlet).

There are complex feedbacks regarding system sizing and costs when the system maximum temperatures are changed. These feedbacks include impacts to the heat exchanger heat transfer, physical sizing, flow rates, the amount of salt required for the desired TES capacity, system heat losses, baffle sizing, and the allowed stress for the hot alloy. It should be noted that this sensitivity is relative to the thermal power going to the power cycle. Changes in power cycle efficiency are not accounted for in the value metric.

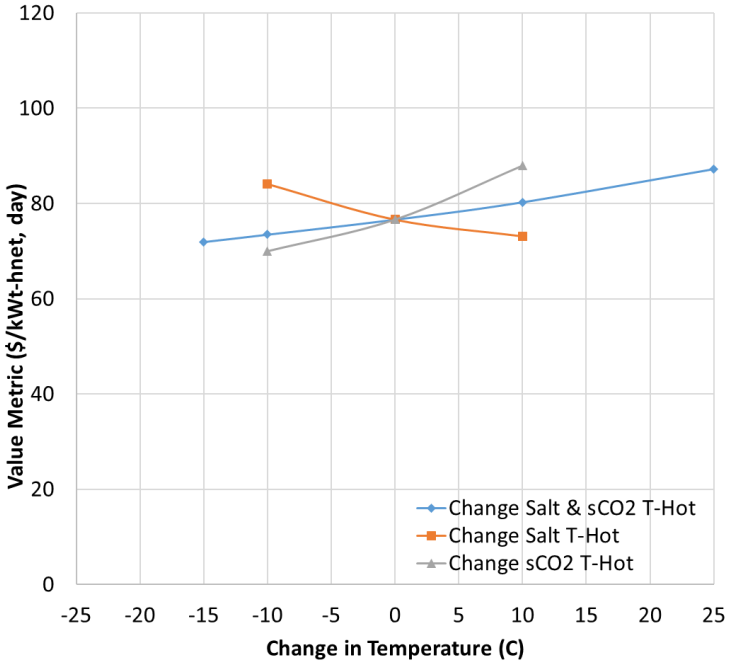

Figure 14. Variation on value metric with system maximum temperature variations.

2.3 POINT DESIGN FOR 5 MWT WITH 12 HOUR TES

The 5 MW_t system with 12 hr TES (60 $MW_{t\text{-}h}$ TES and 100 $MW_{t\text{-}h/day}$ generation and discharge capacity) was chosen as the reference point design. Based on the scoping studies presented in Section 2.2, the HCHX tube's OD was set at 12.7 mm (0.5 in.). Furthermore, the sCO_2 exit velocity from the HCHX was modified to result in a 1 MPa sCO_2 pressure drop across the HCHX. To decrease the overall diameter of components, a tank length-to-diameter ratio of 10 was selected. This would result in the shell, HCHX, and baffle OD being less than 16 ft. Furthermore, the required over-pressure for the design is 14.6 psig, which is less than the 15.0 psig cutoff for various code requirements.

A summary of the chloride salt point design is summarized in Table 6. A more detailed summary of the 0-D model input and output for the 5 MW_t point design with 12-hour TES is provided in Appendix A. The volumes and masses of the required materials are provided in Table 7. Based on the raw material costs provided in Table 3, the estimated component costs and material costs are summarized in Table 8 and Table 9.

The fractions of system mass and cost for each of the major components are summarized in Table 8. As expected, the mass of the salt dominates the mass of the system followed by the mass of the thermocline tank. Interestingly, the predicted material cost of the baffle is substantial. The baffle is a relatively large structure with an inner metal wall made of the high nickel alloy. As modeled, the baffle was designed to resist a pressure differential of 15 psig across each wall during operation. The required wall thickness requires a substantial amount of the high-temperature, high-cost alloy. The high-performance microporous insulation also contributes to 25% of the overall baffle material cost, as seen in Table 7. The other major cost contributors—the HCHX and the thermocline tank—were expected.

The value metric was reduced (i.e., improved) from 76.6 $/$kWt_{net}$-h for the initial 5 MW_t design (see Table 5) to 58.4 $/$kWt_{net}$-h for the chosen point design. Additional component and system optimization of the baffle and HCHX should be explored to reduce system cost further.

Table 6. Summary point design

System size	Nominal discharge power	MWt	5
	Energy storage capacity	MWt-h	60
	Nominal power/day	MWt-h/day	100
	Receiver capacity	MWt	12.5
	Total system height	m	52.0
Tank detail	Tank height	m	50.6
	Shell outer diameter	m	4.8
	Shell thickness (max)	mm	22.5
	Bottom head thickness	mm	18.0
	Top head thickness	mm	3.2
	Outside heat loss	MWt-h/day	1.9
	Outer insulation surface temp.	°C	23.1
	Flange outer diameter	m	5.1
	Bolt size	mm	50.8
	Number of bolts	-	75.0
	Overpressure requirement	psig	14.6
Riser pipe	Riser pipe inner diameter	mm	160.8
	Riser pipe total length	m	49.9
Baffle	Baffle outer diameter	m	4.6
	Inner wall thickness	mm	5.3
	Insulation thickness	mm	98.4
	Outer wall thickness	mm	6.1
	Thermocline velocity	mm/s	1.0
Receiver	Total height	m	3.1
	Panel width	m	6.8
	Tube inner diameter	mm	6.9
	Tube thickness	mm	1.3
	N tubes	-	711.0
	Thermal muffler length	m	1.3
HCHX	Tube outer diameter	mm	12.7
	Tube wall thickness	mm	3.7
	Height	m	2.75
	Tube pitch	mm	18.33
	Tubes	-	525
	sCO_2 pressure drop	MPa	1.00
	Salt flow rate	kg/s	24.73
	Salt inlet temperature	°C	725
	Salt outlet temperature	°C	525
	sCO_2 flow rate	kg/s	19.76
	sCO_2 exit velocity	m/s	12.85
	sCO_2 inlet temperature	°C	500
	sCO_2 outlet temperature	°C	700
Mass sum.	High temperature metal mass	tonne	58
	Low termperature metal mass	tonne	171
	Salt mass	tonne	1,450
	Outside insulation mass	tonne	44
	Inside insulation mass	tonne	34
	Total suspended mass	tonne	1,747
	Weighted cost metric	$	5.73E+06
	Value metric nominal	$/kWt-h	57.3
	Value metric w. loss	$/kWt_net -h	58.4

Table 7. Detailed estimate of component masses and material costs

Component	Detail	Volume	Density	Mass	Cost/kg	Cost
		m^3	kg/m^3	kg	$/kg	$
TC tank	Shell	16.37	7,990	130,758	6.60	863,003
TC tank	Shell inside insulation	5.06	430	2,177	17.08	37,168
TC tank	Shell inside sheath	0.26	8,360	2,210	44.00	97,260
TC tank	Top head	0.08	7,990	607	6.60	4,005
TC tank	Top head inside insulation	2.23	430	960	17.08	16,386
TC tank	Top head inside sheath	0.26	8,360	2,210	44.00	97,260
TC tank	Bottom head	0.43	7,990	3,460	6.60	22,839
TC tank	Top head flange	0.30	7,990	2,416	6.60	15,946
TC tank	Outside insulation	339.75	128	43,629	3.33	145,286
Sump tank	Walls	0.05	7,990	367	6.60	2,423
Sump tank	outside insulation	4.65	128	598	3.33	1,990
Baffle	Inner wall	3.52	8,360	29,434	44.00	1,295,081
Baffle	Outer wall	4.00	7,990	31,962	6.60	210,950
Baffle	Insulation	68.31	430	29,373	17.08	501,574
Riser	Pipe	0.22	7,990	1,731	13.2	22,847
Riser	Outer insulation sheath	0.31	8,360	2,613	44.00	114,973
Riser	Insulation	4.25	430	1,828	17.08	31,218
HCHX	Tube coils	1.99	8,360	16,618	88.00	1,462,353
HCHX	Support material	0.50	8,360	4,154	44.00	182,794
Receiver	Tubes	0.07	8,360	614	88.00	54,067
Receiver	Cold inlet pipe	0.00	7,990	16	13.20	207
Receiver	Plenum pipe	0.02	8,360	158	88.00	13,871
Receiver	Hot return pipe	0.01	8,360	83	88.00	7,293
Salt	Salt	868.46		1,446,346	0.35	506,221
Salt	Magnesium			3,616	2.50	19,887
Totals				**1,757,938**		**5,726,902**

Table 8. Major component mass and cost fraction

Component	Mass fraction	Cost fraction
TC tank	10.7%	22.7%
Sump tank	0.1%	0.1%
Baffle	5.2%	35.1%
Riser	0.4%	3.0%
HCHX	1.2%	28.7%
Receiver	0.0%	1.3%
Salt	82.5%	9.2%

Table 9. Raw material mass, mass fraction, and cost fraction

Raw material	Mass total (kg)	Mass fraction	Cost fraction
Hot alloy (617) - plate/sheet	40,622	2.3%	31.2%
Hot alloy (617) - tube/pipe	17,473	1.0%	26.8%
Cold alloy (316H) - plate/sheet	169,571	9.6%	19.5%
Cold alloy (316H) - tube/pipe	1,746	0.1%	0.4%
Inside insulation (microporous)	34,337	2.0%	10.2%
Outside insulation (mineral wool)	44,227	2.5%	2.6%
Salt (including magnesium)	1,449,962	82.5%	9.2%

A recent report by Turchi et al. was released summarizing a Gen3 CSP pilot plant design [5]. In the study, the high- temperature nickel alloy piping was listed as 80 $/kg, the austenitic stainless steel cold temperature alloy was assumed to cost 8 $/kg, and the salt (delivered and melted) was listed as 0.7 $/kg. The value metric for the point design was re-evaluated with these alternate costs. The value metric decreased slightly with the different cost model, as shown in Table 10.

Table 10. Value metric for alternate cost model

Material	Assumed cost model $/kg	Alternate cost model $/kg
Hot alloy plate/sheet	44.00	40.00
Hot alloy tube/pipe	88.00	80.00
Cold alloy plate/sheet	6.60	4.00
Cold alloy tube/pipe	13.20	8.00
Outside insulation	3.33	3.33
Inside insulation	17.08	17.08
Salt	0.35	0.70
Magnesium	2.5	2.5
Value metric result ($/kW$_{t_net\ -h}$)	**58.4**	**55.9**

2.3.1 Bill of Materials for Point Design

The totals for the required raw materials are noted in Table 9. In addition to these raw materials, metal flashing/weather guard to encase the outside insulation should be included, as well as the materials for the foundation and structural tower. As noted earlier, the sCO_2 power cycle, onsite utilities, and heliostat field are also required.

The theoretical pumping power for the single cold salt pump is low at 1.21 kW (1.6 hp), stemming from the low required head, 33 kPa (6.6 ft). However, the volume flow rate is substantial at 2,227 lpm (588 gpm). Redesign of the receiver to optimize heat transfer may increase the head requirement. The salt pump would be a short-shafted single-stage cantilevered style made of the cold alloy.

The ullage gas system would require approximately 750 liters of gas at standard temperature and pressure to raise the salt from the TC tank into the sump tank. For perspective, a typical 300 ft^3 class high-pressure

gas cylinder holds approximately 8,500 liters of gas. As discussed in Section 1.2.10, the nitrogen system could be an open or closed cycle. Assuming a closed system, a small compressor and two gas tanks would be needed. The system should be constructed of stainless steel, and ¾- inch pipe would be sufficient. At least three pressure relief valves that are capable of elevated temperature service should be included in the gas system. Four actuated valves for the gas lines would be needed, two of which should be rated for high temperatures. A total of six gas pressure transducers would be needed to monitor the two gas tanks (1× each), the sump tank (1× with 1× redundant), and TC tank (1× with 1× redundant). A makeup gas supply in the form of a pressurized gas cylinder should be included; this would require regulator, pressure relief, and isolation valves.

Trace heating around the diameter of the TC tank would be required. Two double-ended tubular heaters could be held in tension with springs around the diameter of the tank shell to maintain good contact. The required tubular heaters are readily within the lengths, voltage, current, and temperature capabilities of multiple commercial suppliers. Dividing the vessel, which is approximately 50 m long, into zones of 2 m each, would result in 25 zones. An additional 7 zones should be included for the top head, bottom head, sump tank, and the riser pipe between the two tanks. Finally, the receiver and associated supply and return piping would add another 6 zones. Assuming 2× the anticipated heat loss of the system, the trace heating system should be sized for approximately 150 kW. However, additional guard heating would likely be required around the receiver.

Approximately 150 thermocouples would be needed: 76 allocated for the trace heating zone, and 74 to monitor the salt temperature within the tanks, HCHX, and receiver. As discussed in Section 1.2.12, a control device is needed to regulate salt flow into the HCHX. Additional optional instrumentation and control could include two liquid level gauges for the sump tank and TC tanks. A salt flow meter is not required, but it would provide a confirmatory measure of pump operation. An electrochemical probe is recommended to monitor the salt potential and the concentration of possible corrosion products in the salt. A gas composition monitor could be added to the ullage gas system to monitor for air leakage into the system.

3. NITRATE SALT SYSTEM POINT DESIGN

3.1 INTRODUCTION

As noted in Section 1.1.1, nitrate salt-based systems are the current deployed state-of-the-art CSP plants. The proposed concept could be adapted to use nitrate salts. The proposed concept's simpler, modular design could result in cost and reliability improvements over the current systems. Thus, the potential application of the proposed concept to nitrate salt systems was explored by leveraging the model and analysis method described in Section 2.1.

3.2 METHODOLOGY

The model, imposed constraints, and assumptions were the same as those described in Section 2.1 except for the following changes.

The hot alloy material was switched to 347 stainless steel, and SA 285-C steel was used as the cold alloy. The salt properties for nitrate-based solar salt were used, as shown in Table 3. The assumed costs for the various materials are provided in Table 11. The TES tank length-to-diameter ratio was assumed to be 8. The cold salt temperature was assumed to be 290°C, and the hot salt temperature was set to 565°C. The model assumed that an sCO_2 power cycle was attached to the tube-side of the HCHX. The sCO_2 inlet temperature was set to 265°C, and the outlet target temperature was 540°C. The nitrate salt system may be more amenable to a supercritical steam cycle, but development of an HCHX model for steam was beyond the scope of the current effort. With the cold-side temperature lower than that of the chloride salt system, the outside insulation thickness was reduced from 0.4 to 0.2 m.

Table 11. Assumed material densities and prices for the nitrate system cost metric

Material	Density	Assigned cost	
	kg/m^3	$/kg	$/lb
Hot alloy plate/sheet	7,960	6.60	3.00
Hot alloy tube/pipe	7,960	13.20	6.00
Cold alloy plate/sheet	7,800	3.30	1.50
Cold alloy tube/pipe	7,800	6.60	3.00
Outside insulation	128	3.33	1.51
Inside insulation	430	17.08	7.76
Salt	*See Table 3*	0.80	0.36

3.3 RESULTS AND COMPARISON TO CHLORIDE SALT POINT DESIGN

The point design is summarized in Table 12, and mass and estimated material costs are presented in Table 13 and Table 14. Appendix A includes a detailed summary of the model input and results.

The temperature difference within the nitrate system TES is 275°C, which is higher than the 200°C temperature difference assumed for the chloride salt system. With the assumed temperature difference and the material properties highlighted in Table 3, the nitrate salt TES stores approximately 700 MJ/m$^3_{salt}$, while the chloride salt TES stores approximately 315 MJ/m$^3_{salt}$ (evaluated using the density of the hot salt). The combination of the difference in salt properties, higher TES temperature gradient, and thinner outside insulation results in a much more compact system for the nitrate salt system than the chloride salt system. The tank height and diameter, salt mass, and system mass are all smaller for the nitrate system.

Using less expensive alloys and less material results in a substantially better value metric for the nitrate system at 17.3 $/kW$_{tnet-h}$ compared to the chloride salt point design at 58.2 $/kW$_{tnet-h}$.

However, comparisons between the nitrate and chloride salt point designs require caution. As noted above, this preconceptual design does not account for many of the expected costs, including site preparation, superstructure and foundation, financing, utilities, instrumentation, component fabrication and shipping, construction, and many other costs. Although many of these costs would be the same for the nitrate salt system or potentially less (e.g., lower temperature instrumentation, smaller components, cheaper fabrication of alloys), this study and comparison do not account for the difference in power cycle thermal efficiency between the two systems. The chloride salt system with the higher operating temperature would have a higher power cycle thermal efficiency than the nitrate system. For example, assuming cycle efficiencies of 33 and 50% for the nitrate and chloride salt systems, respectively, and adding 62 $/kW$_{tnet-h}$ of additional costs not considered for both point designs, the resultant value metric with respect to electrical output ($/kW$_{e-h}$) would be equal between the two systems.

Table 12. Summary point design for nitrate system

System size	Nominal discharge power	MWt	**5**
	Energy storage capacity	MWt-h	**60**
	Nominal power/day	MWt-h/day	**100**
	Receiver capacity	MWt	12.5
	Total system height	m	36.5
Tank detail	Tank height	m	35.1
	Shell outer diameter	m	4.1
	Shell thickness (max)	mm	14.7
	Bottom head thickness	mm	12.0
	Top head thickness	mm	3.2
	Outside heat loss	MWt-h/day	0.8
	Outside insulation surface temperature	°C	22.5
	Flange outer diameter	m	4.4
	Bolt size	mm	44.5
	Number of bolts	-	74.0
	Overpressure requirement	psig	14.2
Riser pipe	Riser pipe inner diameter	mm	111.8
	Riser pipe total length	m	34.6
Baffle	Baffle outer diameter	m	4.0
	Inner wall thickness	mm	3.8
	Insulation thickness	mm	146.1
	Outer wall thickness	mm	6.5
	Thermocline velocity	mm/s	0.6
Receiver	Total height	m	7.1
	Panel width	m	2.9
	Tube inner diameter	mm	6.9
	Tube thickness	mm	1.3
	N tubes	-	308.0
	Thermal muffler length	m	1.1

Table 12. Summary point design for nitrate system (continued)

HCHX	Tube outer diameter	mm	12.7
	Tube wall thickness	mm	3.0
	Height	m	3.10
	Tube pitch	mm	18.33
	Tubes	-	257
	sCO_2 pressure drop	MPa	0.99
	Salt flow rate	kg/s	11.75
	Salt inlet temp	°C	565
	Salt outlet temp	°C	290
	sCO_2 flow rate	kg/s	14.37
	sCO_2 exit velocity	m/s	12.30
	sCO_2 inlet temp	°C	265
	sCO_2 outlet temp	°C	540
Mass summary	High T metal mass	tonne	33
	Low T metal mass	tonne	72
	Salt mass	tonne	792
	Outside insulation mass	tonne	13
	Inside insulation mass	tonne	29
	Total suspended mass	tonne	934
	Weighted cost metric	$	1.72E+06
	Value metric nominal	$/kWt-h	17.2
	Value metric weight loss	$/kWt_net -h	17.3

Table 13. Detailed estimate of component masses and material costs for nitrate system

Component	Detail	Volume	Density	Mass	Cost/kg	Cost
		m^3	kg/m^3	kg	$/kg	$
TC tank	Shell	6.287	7,800	49,042	3.30	161,838
TC tank	Shell inside insulation	6.988	430	3,005	17.08	51,314
TC tank	Shell inside sheath	0.177	7,960	1,405	6.60	9,276
TC tank	Top head	0.056	7,800	437	3.30	1,443
TC tank	Top head inside insulation	2.351	430	1,011	17.08	17,264
TC tank	Top head inside sheath	0.177	7,960	1,405	6.60	9,276
TC tank	Bottom head	0.212	7,800	1,655	3.30	5,463
TC tank	Top head flange	0.199	7,800	1,549	3.30	5,111
TC tank	Outside insulation	97.974	128	12,582	3.33	41,897
Sump tank	Walls	0.036	7,800	277	3.30	915
Sump tank	Outside insulation	1.622	128	208	3.33	694
Baffle	Inner wall	1.453	7,960	11,563	6.60	76,313
Baffle	Outer wall	2.375	7,800	18,529	3.30	61,145
Baffle	Insulation	53.659	430	23,073	17.08	393,998
Riser	Pipe	0.0843	7,800	657	6.60	4,338
Riser	Outer insulation sheath	0.175	7,960	1,396	6.60	9,214
Riser	Insulation	4.300	430	1,849	17.08	31,573
HCHX	Tube coils	1.627	7,960	12,950	13.20	170,936
HCHX	Support material	0.407	7,960	3,237	6.60	21,367
Receiver	Tubes	0.073	7,960	585	13.20	7,722
Receiver	Cold inlet pipe	0.001	7,800	8	6.60	54
Receiver	Plenum pipe	0.008	7,960	65	13.20	858
Receiver	Hot return pipe	0.005	7,960	37	13.20	494
Salt	Salt	439.302		792,298	0.80	633,838
Totals				**938,824**		**1,716,339**

Table 14. Major component mass and cost fraction for nitrate system

	Mass fraction	Cost fraction
TC tank	7.7%	17.6%
Sump tank	0.1%	0.1%
Baffle	5.7%	31.0%
Riser	0.4%	2.6%
HCHX	1.7%	11.2%
Receiver	0.1%	0.5%
Salt	84.4%	36.9%

4. DEVELOPMENT ROADMAP

4.1 CONCEPT MATURATION

4.1.1 Subcomponent Analysis, Design, and Demonstration

The point design has not been optimized for cost or performance. More rigorous, higher fidelity models for the system and subcomponents should be developed with a focus on the following areas:

1. Stability and performance of the thermocline should be investigated further through detailed computational analysis. The limited information available is promising (see Section 1.2.1), but stability of the thermocline is essential for the concept. The stability analysis should consider heat transfer along the walls in the system, potential formation of convection cells, and the impact of planned and unplanned system transients.

2. Although a modest effort was expended to model the HCHX, it should be noted that the component is complex, with tightly coupled thermal hydraulic, structural, and fabrication considerations. As noted in Section 2.3, the HCHX comprises approximately 29% of the system material cost considered. A more rigorous design and analysis of the HCHX is recommended.

3. The baffle comprises 35% of the system material cost considered. In contrast to the HCHX, the baffle has a relatively simple design. However, given its substantial impact on the overall cost and value metric, refinement of the baffle design is recommended.

Some components may warrant testing prior to committing to a larger scale demonstration. Three items that may warrant further investigation are (1) the stability of the thermocline, (2) characterization of the low salt flow HCHX performance, and (3) baffle design and performance.

4.1.2 Detailed Plant Modeling

The proposed concept would be further informed by a system model that can analyze system feedback and performance during transient scenarios. Transients of interest include start-up, diurnal insolation variation, rapid and intermittent variations in insolation, changing environment conditions, and disruptions to the charge/discharge cycle. This model would provide insight into system stability and would inform the control and operation scheme.

4.1.3 Detailed System Conceptual Design

This study should be used as a starting point to develop and optimize a detailed system design to obtain performance and cost metrics. This effort would include defining the salt system design and the integrated sCO_2 power cycle, heliostat field, and civil structures. The detailed design could then be used to develop a more rigorous cost estimate to evaluate the concept's potential economic viability.

4.2 1-5 MW_t DEMONSTRATION

The National Solar Thermal Test Facility at Sandia National Laboratories includes a 61 m (200 ft) tower and a multi-megawatt heliostat field. A demonstration unit could be contained within and supported by the existing tower. A larger demonstration could be built alongside the tower. Key areas for demonstration include transient operation characteristics, thermocline stability, and real-world operation experience in an integral system of relevant scale. This type of demonstration would not likely require a full 12-hour TES capacity. Beyond demonstrating the integrated system and subcomponents, the

demonstration unit could be used to optimize components such as the receiver HCHX that would be difficult to study on a smaller scale or without integration into an integral system.

4.3 PILOT PLANT

As noted in the introduction (Section 3.1), a 10 MW_e sCO_2 power cycle is being constructed at the Southwest Research Institute under the STEP program [6]. A commercial pilot plant could be created by coupling 5 of the 5 MW_t modules to a sCO_2 power cycle of similar size as that being demonstrated under STEP. Furthermore, a sixth module could be constructed to allow for isolation of a single module from the system for inspection and maintenance.

Outside the STEP program, smaller (i.e., <10 Mwe) sCO_2 power cycles are also under development by industrial entities. A ~2.5 MW_e power cycle coupled with a 5 MW_t module could be built and operated while another module is under construction.

Beyond demonstrating the technology at a pilot plant scale, the facility could be used to explore and demonstrate different system architectures (e.g., number of units banked with power cycle) and operation schemes (e.g., sequential vs. parallel discharge of module TES).

5. REFERENCES

1. Islam, M. T., et al., "A Comprehensive Review of State-of-the-Art Concentrating Solar Power (CSP) Technologies: Current Status and Research Trends." *Renewable and Sustainable Energy Reviews* 91 (2018): 987–1018.
2. Boretti, A., Castelletto, S., and Al-Zubaidy, S., "Concentrating Solar Power Tower Technology: Present Status and Outlook." *Nonlinear Eng.* 8.1 (2019): 10–31.
3. Mehos, M., et al., *Concentrating Solar Power Gen3 Demonstration Roadmap*. NREL/TP-5500-67464. National Renewable Energy Laboratory (NREL), Golden, CO, 2017.
4. Price, H., Mehos, M. S., Cable, R., Kearney, D., Kelly, B., Kolb, G., and Morse, F., "CSP Plant Construction, Start-Up, and O&M Best Practices Study." In *AIP Conf. Proc.* Vol. 2303, No. 1, (2020): 040002). AIP Publishing LLC.
5. Turchi, C., et al., *CSP Gen3: Liquid-Phase Pathway to SunShot*. NREL/TP-5700-79323. National Renewable Energy Laboratory (NREL), Golden, CO (2021).
6. Marion, J., Kutin, M., McClung, A., Mortzheim, J., and Ames, R., "The STEP 10 MWe sCO_2 Pilot Plant Demonstration." *Proc. ASME Turbo Expo 2019: Turbomachinery Technical Conference and Exposition.* Vol. 9, Oil and Gas Applications; Supercritical CO_2 Power Cycles; Wind Energy. Phoenix, Arizona (June 17–21, 2019). V009T38A031. ASME. https://doi.org/10.1115/GT2019-91917
7. Alfani, D., et al., "Multi Objective Optimization of Flexible Supercritical CO_2 Coal-Fired Power Plants." *ASME Turbo Expo 2019: Turbomachinery Technical Conference and Exposition*. American Society of Mechanical Engineers Digital Collection (2019).
8. Seubert, B., et al., "Experimental Results from a Laboratory-Scale Molten Salt Thermocline Storage." AIP Conf. Proc. 1850. 1. AIP Publishing LLC (2017).
9. Pacheco, J. E., Showalter, S. K., and Kolb, W. J., "Development of a Molten-Salt Thermocline Thermal Storage System for Parabolic Trough Plants." *J. Sol. Energy Eng.* 124.2 (2002): 153–159.
10. Kim, D. H., et al., "Experimental Studies on the Charging Performance of Single-Tank Single-Medium Thermal Energy Storage." *Appl. Therm. Eng.* 149 (2019): 1098–1104.
11. Odenthal, C., Klasing, F., and Bauer, T., "Experimental and Numerical Investigation of a 4 MWh Single Tank Thermocline Storage." Poster, Proc. SolarPACES, 2018. https://elib.dlr.de/123716/1/2018-10%20SolarPaces%202018_Odenthal.pdf
12. Kelly, B. D., *Advanced Thermal Storage for Central Receivers with Supercritical Coolants*, DE-FG36-08GO18149, US Department of Energy: N. p. (2010). Web. doi:10.2172/981926.
13. "Dangote Refinery Receives World's Largest Crude Distillation Equipment," *This Day Live,* https://www.thisdaylive.com/index.php/2019/12/02/dangote-refinery-receives-worlds-largest-crude-distillation-equipment/#:~:text=The%20world's%20largest%20crude%20distillation,650%2C000%20barrels%20per%20stream%20day (accessed March 9, 2022).
14. Nicodemus, J. H., et al., "Effect of Baffle and Shroud Designs on Discharge of a Thermal Storage Tank Using an Immersed Heat Exchanger." *J. Sol. Energy* 157 (2017): 911–919.
15. Robb, K. R., Jain, P. K., and Hazelwood, T. J., *High-Temperature Salt Pump Review and Guidelines—Phase I Report*, ORNL/TM-2016/199, Oak Ridge National Laboratory (May 2016).

16. Yoder Jr., G. L., et al., "An Experimental Test Facility to Support Development of the Fluoride-Salt-Cooled High-Temperature Reactor." *Ann. Nucl. Energy* 64 (2014): 511–517.

17. Robb, K., et al., *Facility to Alleviate Salt Technology Risks (FASTR): Preliminary Design Report with Failure Modes and Effects Analysis*, ORNL/TM-2019/1370, Oak Ridge National Laboratory (ORNL), Oak Ridge, TN (2019).

18. Rockwool ProRox® MA 960NA data sheet, https://rti.rockwool.com/siteassets/tools--documentation/documentation/countries/industrial---usa/datasheets/rti-prorox-ma-960_na_en.pdf (accessed March 4, 2021).

19. Aspen Aerogel Pyrogel® XTE data sheet, https://www.aerogel.com/products-and-solutions/pyrogel-xte/ (accessed March 4, 2021).

20. Zhao, Y., *Molten Chloride Thermophysical Properties, Chemical Optimization, and Purification*. NREL/TP-5500-78047. National Renewable Energy Laboratory (NREL), Golden, CO (2020).

21. Takeuchi, M., et al., "Corrosion Resistance of Ceramic Materials in Pyrochemical Reprocessing Condition by Using Molten Salt for Spent Nuclear Oxide Fuel." *J. Phys. Chem. Solids* 66.2–4 (2005): 521–525.

22. Gage, S. H., et al., "Internal Insulation and Corrosion Control of Molten Chloride Thermal Energy Storage Tanks." *Solar Energy Materials and Solar Cells* 225 (2021): 111048.

23. Gage, S. H., and Turchi, C. S., "Internal Insulation and Corrosion Control of Molten Chloride Storage Tanks." AIP Conf. Proc.. 2303:1. AIP Publishing LLC (2020).

24. Weikl, M. C., Braun, K., and Weiss, J., "Coil-Wound Heat Exchangers for Molten Salt Applications." *Energy Procedia* 49 (2014): 1054–1060.

25. Sohal, M. S., et al., *Engineering Database of Liquid Salt Thermophysical and Thermochemical Properties*. INL/EXT-10-18297. Idaho National Laboratory, (2010).

26. Zavoico, A. B., *Solar Power Tower Design Basis Document*, Revision 0. SAND2001-2100. Sandia National Laboratories, Albuquerque, NM (US), Livermore, CA (2001).

27. NIST Chemistry WebBook, SRD 69, *Thermophysical Properties of Fluid Systems*, https://webbook.nist.gov/chemistry/fluid/ (accessed April 24, 2020).

28. Kakaç, S., Shah, R. K. and Aung, W., *Handbook of Single-Phase Convective Heat Transfer*." N. p. (1987), Web.

APPENDIX A. SUPPLEMENTAL INFORMATION

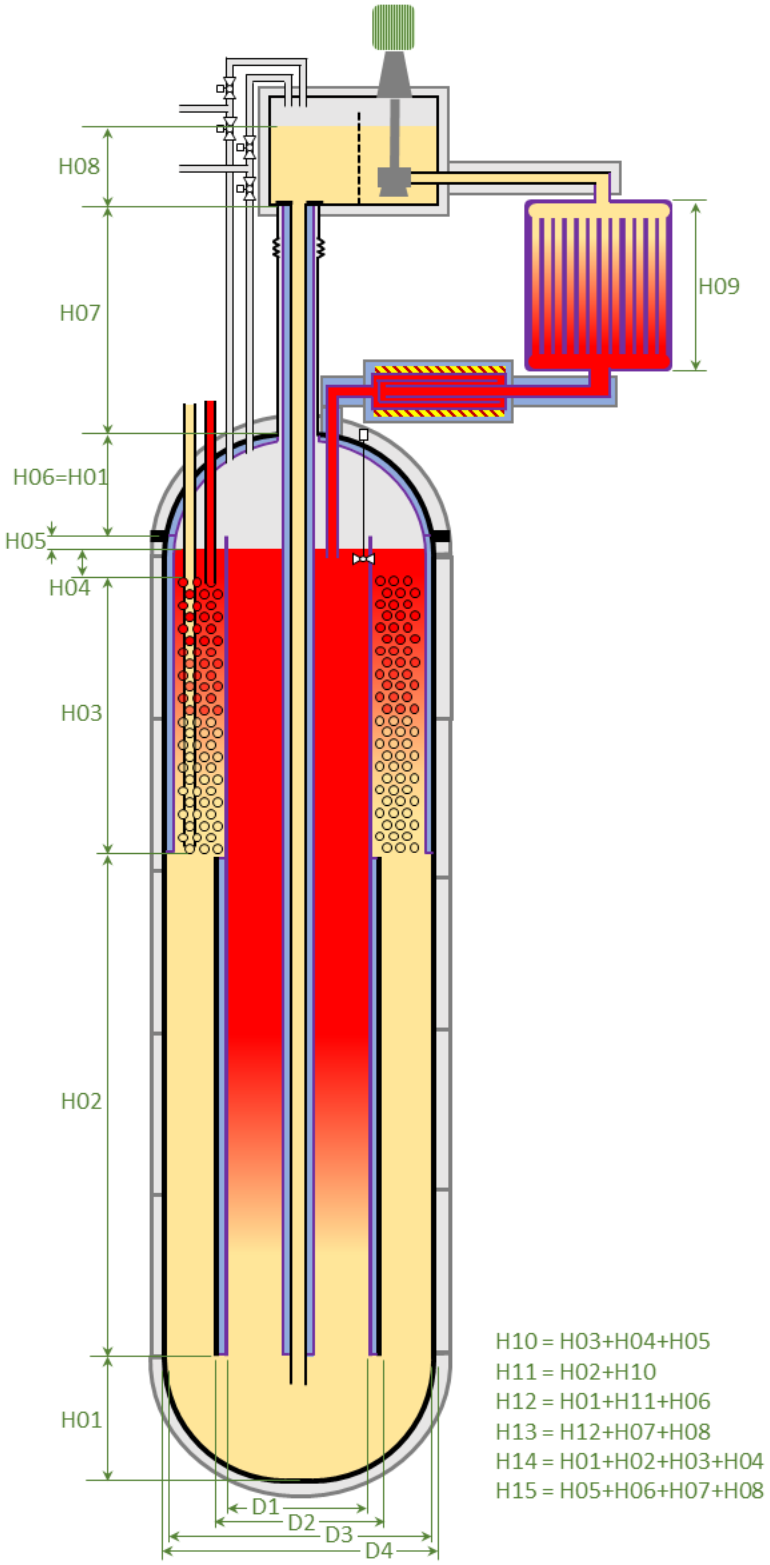

Figure A.1. Concept schematic with dimension notations.

A.1 CHLORIDE SALT 5 MW_T SYSTEM DESIGN MODEL DETAILS

Input Parameters (Yellow)

	Value	Units		
Overall				
Desired MWth to power cycle	**5**	MWt		
Desired E Store duration	12	h		
Charge time (while discharging)	8	h		
Energy storage (TES)	**60**	MWt-h		
Solar multiple	2.5	-		
Required MWth receiver capacity	12.5	MWt		
Total daily power (nominal)	**100**	MWt-h/day		
Desired E storage dT	200	C	392	F
Hot salt temp	725	C	1337	F
Cold salt temp	525	C	977	F
Maximum outer surface temp	57.2	C	135	F
Outside temperature	21.1	C	70	F
Air flow convective coeff	50.0	W/m K		
Shell max OD	5.126	m	**16.816**	ft
Tank				
H08 pump tank salt level	0.60	m	23.62	in
H07 Clearance in. top head & in. pump	0.50	m	19.69	in
H05 gas gap bet. top of salt & flange	0.50	m	19.69	in
H04 Salt above HX	0.25	m	9.84	in
min wall thickness	0.0032	m	0.125	in
operation gas overpressure in thermoc	100.7	kPa-g	14.6	psig
Shell variable or uniform thickness?	0	0=uni, 1=var		
Shell max var. thick segment length	6.0	m	19.7	ft

Output Parameters (Green)

	Value	Units		
Overall				
needed E salt store mass	1068249	kg		
Rho salt at hot temp	1548	kg/m^3		
Rho salt at cold temp	1665	kg/m^3		
Tank				
H12 Total tank height (- insul)	50.60	m	166.0	ft
H11 tank cylinder height	48.19	m	158.1	ft
H10 tank cylinder height, hot face	3.50	m	11.5	ft
H02 tank cylinder height, cold face	44.69	m	146.6	ft
H14 total salt height in TC tank	48.89	m	160.4	ft
**Needed salt height in TC tank	48.89	m	160.4	ft
total baffle length (=H11)	48.19	m	158.1	ft
H02 baffle length below HX	44.69	m	146.6	ft
H01 Bottom salt plenum below baffl	1.205	m	4.0	ft
H13 total salt height to top of pump	51.698	m	169.6	ft
H15 distance between salt free surfa	2.805	m	9.2	ft
Shell L/D	10.00	-		
D4 Tank shell OD (max)	4.821	m	15.816	ft
D3 Tank shell ID	4.776	m	15.67	ft
Max cyl. shell thickness	22.53	mm	0.887	in
Tank shell metal V	16.37	m^3		
top head thickness	0.0032	m	0.125	in
Top head metal V	0.076	m^3		
bottm head thickness	0.0180	m	0.707	in
Bottom head metal V	0.433	m^3		

A-1 CHLORIDE SALT 5 MW_T SYSTEM DESIGN MODEL DETAILS (CONTINUED)

Input Parameters (Yellow)					Output Parameters (Green)				
					Tank top head inner insulation V	2.232	m^3		
					Tank top head inner metal sheath V	0.113	m^3		
					Tank shell inner insulation V	5.062	m^3		
					Tank shell inner metal sheath V	0.264	m^3		
					Head gas space volume (nominal)	23.2	m^3		
Hot material					**Hot material**				
Hot matl design temp margin	10	ΔC	18	ΔF	Design temp	735	C		
Hot matl material number	7	-			Allowed stress at temp.	58.6	MPa	8502	psi
Hot matl material name	617	-			Allowed stress at amb.	161.0	MPa	23351	psi
Hot matl corrosion allowance	30	µm/y	0.0012	in/y	Corrosion allow.	0.900	mm	0.035	in
Hot matl corrosion allowance	30	y			Material density	8360	kg/m^3		
Hot matl joint efficiency	1.00	-							
Cold material					**Cold material**				
Cold wall design temp margin	25	ΔC	45	ΔF	Design temp	550	C		
Cold wall material number	5	-			Allowed stress at temp	105.0	MPa	15229	psi
Cold wall material name	316 >0.04	-			Allowed stress at amb.	138.0	MPa	20015	psi
Cold wall corrosion allowance	30	µm/y	0.0012	in/y	Corrosion allow.	0.900	mm	0.035	in
Cold design life	30	y			Material density	7990	kg/m^3		
Cold wall joint efficiency	0.85	-							
Outside Insulation					**Outside Insulation**				
shell insulation thickness	0.40	m	15.75	in	heat loss rate	99.9	W/m^2		
insulated pre/post shipping?	0	1=pre, 0=post			outer surface temp	23.1	C	73.6	F
insulation material number	1	1=rockwool, 2=pyrogel			heat loss per length	1498	W/m		
					shell heat loss	72204	W		
					shell heat loss % power	1.44%	%		
					insulation density	0.13	g/cc		
					shell insulation volume	316.14	m^3		
					top head insulation volume	11.72	m^3		
					bottom head insulation volume	11.89	m^3		
					total heat loss	729.8	m^2		
					top head area	23.9	m^2		
					bottom head area	24.1	m^2		
					total area	778	m^2		
					total heat loss	77682	W		
					MWh/day loss	1.9	MWh/day loss		
					net power per day	**98.1**	MWh/day		
					loss percent	1.9%	%		

A-1 CHLORIDE SALT 5 MW_T SYSTEM DESIGN MODEL DETAILS (CONTINUED)

Input Parameters (Yellow)				Output Parameters (Green)			
				Thermal efficiency (charge/disch.)	98.1%	%	
Top head flange and bolt				**Top head flange and bolt**			
bolt material number	1	- (1-10)		bolt size required	50.8	mm	2 in
bolt material name	316, SA-193 B8M S31600 Class 1			number of bolts needed	75	-	
bolt spacing	4.0	L/D C-C		flange width	0.1524	m	6.0 in
bolt center to edge distance	1.50	L/D C-E		flange single side thick	0.0635	m	2.5 in
flange/bolt thickness ratio	1.25	T/D E-E		design head gas overpressure	100.7	kPa-g	14.6 psig
assumed seal seat load	482	N/mm	2750 lb/in	flange metal volume (total)	0.302	m^3	
Baffle				**Baffle**			
outer wall material	2	1=hot matl, 2=cold matl		insulation therm. Cond. (mean)	0.051	W/m K	
inner wall material	1	1=hot matl, 2=cold matl		insulation density	0.430	g/cc	
wall design dP (@ high temp)	103.4	kPa-g	15 psig	D2 baffle wall OD	4.649	m	183.02 in
wall design dP (@ room temp)	887.20	kPa-g	128.7 psig	D1 baffle wall ID	4.434	m	174.58 in
baffle bot. hyrdostatic head	887.20	kPa-g	128.7 psig	baffle inner area	15.444	m^2	
min wall thickness	1.59	mm	0.0625 in	outer baffle metal thick	6.1	mm	0.241 in
				inner baffle metal thick	5.3	mm	0.207 in
				insul thickness	0.098	m	**3.875** in
				heat loss per length	1464.3	W/m	
				Annular HCHX area without tubes	3.926	m^2	
				Annular downcomer area	0.940	m^2	
				outer baffle metal volume	4.000	m^3	
				inner baffle metal volume	3.521	m^3	
				baffle insulation volume	68.309	m^3	
Pump and Sump Tank				**Pump and Sump Tank**			
min wall thickness	0.00318	m	0.125 in	Pump theoretical power	1.21	kW	
design gas overpressure in pump tank	34.5	kPa-g	5 psig	Tank ID	2.410	m	94.896 in
				Tank OD	2.417	m	95.146 in
				Shell tank height	0.299	m	11.760 in
				Head height	0.301	m	11.862 in
				Shell thickness	0.00318	m	0.125 in
				Head thickness	0.00318	m	0.125 in
				Tank metal volume	0.0460	m^3	
				shell insulation thickness	1.0573	m^3	
				top and bottom head insul thickness	3.5966	m^3	
Receiver				**Receiver**			
tube OD	9.53E-03	m	0.375 in	Avg salt flow rate during charge	61.82	kg/s	
Assumed heat flux into salt	0.6	MW/m2		cold salt flow rate	2227	lpm	588 gpm

A-1 CHLORIDE SALT 5 MW_T SYSTEM DESIGN MODEL DETAILS (CONTINUED)

Input Parameters (Yellow)					Output Parameters (Green)				
Target intlet Re number	5000	-			Min req. planar heat flux without los	1.370	MW/m^2		
tube design P for wall thickness	206.8	kPa-g	30	psig	Actual inlet Re number	5050	-		
tube design stress for wall	12.3	MPa			Tube inlet velocity	1.414	m/s		
in/out pipe salt velocity	1	m/s			Tube wall thickness	0.001	m	0.051	in
					Tube ID	0.007	m	0.273	in
					number tubes	711			
					panel width	6.77	m		
					panel height	3.08	m		
					tube bank dP	26.9	kPa	3.9	psig
					receiver pipe network total dP	32.7	kPa	4.7	psig
					receiver tube metal volume	0.0735	m^3		
					muffler length	1.281	m		
Riser Pipe					**Riser Pipe**				
					Pipe Length	49.89	m		
					Tube ID	160.799	mm	6.331	in
					Wall thickness	8.18	mm	0.322	in
					Outer sheath thick. (=baffle inner)	5.26	mm	0.207	in
					insulat thickness (= baffle)	98.4	mm	3.9	in
					Outer sheath metal volume	0.313	m^3		
					Pipe metal volume	0.217	m^3		
					Pipe insualtion volume	4.252	m^3		
HCHX					**HCHX**				
Downcomer annulus width	0.0635	m	2.5	in	tube wall thickness	0.00366	m	0.144	in
HCHX annulus width	0.1741	m	6.856	in	tube cross sectional metal area	1.04E-04	m^2		
**needed annulus width	0.1804	m	7.101	in	tube cross sectional fluid area	2.28E-05	m^2		
H03 HX bundle height	**2.75**	m	9.0	ft	Tube bundle outer surf area/row	4.406	m^2/row		
Bundle tube OD	0.0127	m	0.5	in	Rows in axial direction	173.23	rows		
Support mat. Fraction (Coil x Frac.)	0.25	-			Total tube outer surface area	763.29	m^2		
tube count in bundle (across width)	8	number			Total tube inner surface area	323.63	m^2		
sCO2 exit velocity	**12.85**	m/s			tube stress (pre corrosion)	43.4	Mpa	6.3	ksi
sCO2 cp	1265	J/kg k			tube metal volume coil	1.988	m^3		
sCO2 mdot	19.8	kg/s			support metal volume	0.497	m^3		
**Needed sCO2 flow rate	19.8	kg/s			approx. volume of salt	868	m^3		
sCO2 exit temp	700	C			approx. mass of salt	1446346	kg		
desired sCO2 inlet temp	500	C			total tube twists	2.6	-		
sCO2 pressure	25	Mpa			tubes per bundle	525.0	-		
salt cp	1011	J/kg k			sCO2 dP	1.00	MPa	145	psi

A-1 CHLORIDE SALT 5 MW_T SYSTEM DESIGN MODEL DETAILS (CONTINUED)

Input Parameters (Yellow)

Salt mdot	24.73	kg/s
**Needed salt mdot	24.73	kg/s over X h
salt node dT transition	20	

Output Parameters (Green)

sCO2 dP goal	1.0-0.9	MPa		
HCHX annulus ID	4.22	m		
Actual stored E	215989	MJ		
Actual stored E	60.0	MW-h		
Goal stored E	60.0	MW-h		
Actual total power	5.0	MW		
Goal total power	5.0	MW		
Actual salt cold temp	525.0	C		
Goal salt cold temp	525	C		
sCO2 inlet temp	500.0	C		
Goal sCO2 inlet temp	>475	C		
flow rate of salt in TC	1.0344	mm/s		
Driving dP	47.9	kPa	6.95	psig
Pressure loss	0.399	kPa	0.06	psig

A.2 NITRATE SALT 5 MW_T SYSTEM DESIGN MODEL DETAILS

Input Parameters (Yellow)

	Value	Units		
Overall				
Desired MWth to power cycle	**5**	MWt		
Desired E Store duration	12	h		
Charge time (while discharging)	8	h		
Energy storage (TES)	**60**	MWt-h		
Solar multiple	2.5	-		
Required MWth receiver capacity	12.5	MWt		
Total daily power (nominal)	**100**	MWt-h/day		
Desired E storage dT	275	C	527	F
Hot salt temp	565	C	1049	F
Cold salt temp	290	C	554	F
Maximum outer surface temp	57.2	C	135	F
Outside temperature	21.1	C	70	F
Air flow convective coeff	50.0	W/m K		
Shell max OD	4.398	m	**14.43**	ft
Tank				
H08 pump tank salt level	0.60	m	23.62	in
H07 Clearance in. top head & in. pump	0.50	m	19.69	in
H05 gas gap bet. top of salt & flange	0.50	m	19.69	in
H04 Salt above HX	0.25	m	9.84	in
min wall thickness	0.0032	m	0.125	in
operation gas overpressure in thermoc	98.1	kPa-g	14.2	psig
Shell variable or uniform thickness?	0	0=uni, 1=var		
Shell max var. thick segment length	6.0	m	19.7	ft

Output Parameters (Green)

	Value	Units		
Overall				
needed E salt store mass	507400	kg		
Rho salt at hot temp	1642	kg/m^3		
Rho salt at cold temp	1804	kg/m^3		
Tank				
H12 Total tank height (- insul)	35.12	m	115.2	ft
H11 tank cylinder height	33.06	m	108.4	ft
H10 tank cylinder height, hot face	3.85	m	12.6	ft
H02 tank cylinder height, cold face	29.21	m	95.8	ft
H14 total salt height in TC tank	33.59	m	110.2	ft
**Needed salt height in TC tank	33.61	m	110.3	ft
total baffle length (=H11)	33.06	m	108.4	ft
H02 baffle length below HX	29.21	m	95.8	ft
H01 Bottom salt plenum below baffl	1.033	m	3.4	ft
H13 total salt height to top of pump	36.221	m	118.8	ft
H15 distance between salt free surfa	2.633	m	8.6	ft
Shell L/D	8.00	-		
D4 Tank shell OD (max)	4.132	m	13.555	ft
D3 Tank shell ID	4.102	m	13.46	ft
Max cyl. shell thickness	14.71	mm	0.579	in
Tank shell metal V	6.29	m^3		
top head thickness	0.0032	m	0.125	in
Top head metal V	0.056	m^3		
bottm head thickness	0.0120	m	0.471	in
Bottom head metal V	0.212	m^3		

A.2 NITRATE SALT 5 MWT SYSTEM DESIGN MODEL DETAILS (CONTINUED)

Input Parameters (Yellow)					Output Parameters (Green)				
					Tank top head inner insulation V	2.351	m^3		
					Tank top head inner metal sheath V	0.056	m^3		
					Tank shell inner insulation V	6.988	m^3		
					Tank shell inner metal sheath V	0.177	m^3		
					Head gas space volume (nominal)	15.6	m^3		
Hot material					**Hot material**				
Hot matl design temp margin	10	ΔC	18	ΔF	Design temp	575	C		
Hot matl material number	4	-			Allowed stress at temp.	77.2	MPa	11197	psi
Hot matl material name	347	-			Allowed stress at amb.	138.0	MPa	20015	psi
Hot matl corrosion allowance	30	µm/y	0.0012	in/y	Corrosion allow.	0.900	mm	0.035	in
Hot matl corrosion allowance	30	y			Material density	7960	kg/m^3		
Hot matl joint efficiency	0.85	-							
Cold material					**Cold material**				
Cold wall design temp margin	25	ΔC	45	ΔF	Design temp	315	C		
Cold wall material number	11	-			Allowed stress at temp	105.2	MPa	15258	psi
Cold wall material name	SA-285 C	-			Allowed stress at amb.	108.0	MPa	15664	psi
Cold wall corrosion allowance	30	µm/y	0.0012	in/y	Corrosion allow.	0.900	mm	0.035	in
Cold design life	30	y			Material density	7800	kg/m^3		
Cold wall joint efficiency	0.85	-							
Outside Insulation					**Outside Insulation**				
shell insulation thickness	0.20	m	7.87	in	heat loss rate	69.7	W/m^2		
insulated pre/post shipping?	0	1=pre, 0=post			outer surface temp	22.5	C	72.5	F
insulation material number	1	1=rockwool, 2=pyrogel			heat loss per length	899	W/m		
					shell heat loss	29709	W		
					shell heat loss % power	0.59%	%		
					insulation density	0.13	g/cc		
					shell insulation volume	89.96	m^3		
					top head insulation volume	3.99	m^3		
					bottom head insulation volume	4.03	m^3		
					total heat loss	429.0	m^2		
					top head area	17.7	m^2		
					bottom head area	17.8	m^2		
					total area	464	m^2		
					total heat loss	32391	W		
					MWh/day loss	0.8	MWh/day loss		
					net power per day	**99.2**	MWh/day		
					loss percent	0.8%	%		

A.2 NITRATE SALT 5 MWT SYSTEM DESIGN MODEL DETAILS (CONTINUED)

Input Parameters (Yellow)					Output Parameters (Green)				
					Thermal efficiency (charge/disch.)	99.2%	%		
Top head flange and bolt					**Top head flange and bolt**				
bolt material number	1	- (1-10)			bolt size required	44.45	mm	1.75	in
bolt material name	316, SA-193 B8M S31600 Class 1				number of bolts needed	74	-		
bolt spacing	4.0	L/D C-C			flange width	0.13335	m	5.3	in
bolt center to edge distance	1.50	L/D C-E			flange single side thick	0.055563	m	2.1875	in
flange/bolt thickness ratio	1.25	T/D E-E			design head gas overpressure	98.1	kPa-g	14.2	psig
assumed seal seat load	482	N/mm	2750	lb/in	flange metal volume (total)	0.199	m^3		
Baffle					**Baffle**				
outer wall material	2	1=hot matl, 2=cold matl			insulation therm. Cond. (mean)	0.039	W/m K		
inner wall material	1	1=hot matl, 2=cold matl			insulation density	0.430	g/cc		
wall design dP (@ high temp)	103.4	kPa-g	15	psig	D2 baffle wall OD	3.975	m	156.50	in
wall design dP (@ room temp)	682.35	kPa-g	99.0	psig	D1 baffle wall ID	3.669	m	144.45	in
baffle bot. hyrdostatic head	682.35	kPa-g	99.0	psig	baffle inner area	10.573	m^2		
min wall thickness	1.59	mm	0.0625	in	outer baffle metal thick	6.5	mm	0.256	in
					inner baffle metal thick	3.8	mm	0.151	in
					insul thickness	0.146	m	**5.750**	in
					heat loss per length	889.4	W/m		
					Annular HCHX area without tubes	3.846	m^2		
					Annular downcomer area	0.806	m^2		
					outer baffle metal volume	2.375	m^3		
					inner baffle metal volume	1.453	m^3		
					baffle insulation volume	53.659	m^3		
Pump and Sump Tank					**Pump and Sump Tank**				
min wall thickness	0.00318	m	0.125	in	Pump theoretical power	1.03	kW		
design gas overpressure in pump tank	34.5	kPa-g	5	psig	Tank ID	2.066	m	81.330	in
					Tank OD	2.072	m	81.580	in
					Shell tank height	0.342	m	13.456	in
					Head height	0.258	m	10.166	in
					Shell thickness	0.00318	m	0.125	in
					Head thickness	0.00318	m	0.125	in
					Tank metal volume	0.0355	m^3		
					shell insulation thickness	0.4879	m^3		
					top and bottom head insul thickness	1.1345	m^3		
Receiver					**Receiver**				
tube OD	9.53E-03	m	0.375	in	Avg salt flow rate during charge	29.36	kg/s		
Assumed heat flux into salt	0.6	MW/m2			cold salt flow rate	977	lpm	258	gpm

A.2 NITRATE SALT 5 MWT SYSTEM DESIGN MODEL DETAILS (CONTINUED)

Input Parameters (Yellow)				Output Parameters (Green)				
Target intlet Re number	5000	-		Min req. planar heat flux without los	1.370	MW/m^2		
tube design P for wall thickness	206.8	kPa-g	30 psig	Actual inlet Re number	5255	-		
tube design stress for wall	12.3	MPa		Tube inlet velocity	1.332	m/s		
in/out pipe salt velocity	1	m/s		Tube wall thickness	0.001	m	0.051	in
				Tube ID	0.007	m	0.273	in
				number tubes	308			
				panel width	2.93	m		
				panel height	7.10	m		
				tube bank dP	57.1	kPa	8.3	psig
				receiver pipe network total dP	63.5	kPa	9.2	psig
				receiver tube metal volume	0.0735	m^3		
				muffler length	1.100	m		
Riser Pipe				**Riser Pipe**				
				Pipe Length	34.59	m		
				Tube ID	111.788	mm	4.401	in
				Wall thickness	6.55	mm	0.258	in
				Outer sheath thick. (=baffle inner)	3.84	mm	0.151	in
				insulat thickness (= baffle)	146.1	mm	5.8	in
				Outer sheath metal volume	0.175	m^3		
				Pipe metal volume	0.084	m^3		
				Pipe insualtion volume	4.300	m^3		
HCHX				**HCHX**				
Downcomer annulus width	0.0635	m	2.5 in	tube wall thickness	0.00300	m	0.118	in
HCHX annulus width	0.1741	m	6.856 in	tube cross sectional metal area	9.14E-05	m^2		
**needed annulus width	0.1804	m	7.101 in	tube cross sectional fluid area	3.53E-05	m^2		
H03 HX bundle height	**3.1**	m	10.2 ft	Tube bundle outer surf area/row	3.638	m^2/row		
Bundle tube OD	0.0127	m	0.5 in	Rows in axial direction	195.28	rows		
Support mat. Fraction (Coil x Frac.)	0.25	-		Total tube outer surface area	710.46	m^2		
tube count in bundle (across width)	8	number		Total tube inner surface area	375.12	m^2		
sCO2 exit velocity	**12.3**	m/s		tube stress (pre corrosion)	53.0	Mpa	7.7	ksi
sCO2 cp	1265	J/kg k		tube metal volume coil	1.627	m^3		
sCO2 mdot	14.4	kg/s		support metal volume	0.407	m^3		
**Needed sCO2 flow rate	14.4	kg/s		approx. volume of salt	439	m^3		
sCO2 exit temp	540	C		approx. mass of salt	792298	kg		
desired sCO2 inlet temp	265	C		total tube twists	6.1	-		
sCO2 pressure	25	Mpa		tubes per bundle	257.2	-		
salt cp	1548	J/kg k		sCO2 dP	0.99	MPa	143	psi

A.2 NITRATE SALT 5 MWT SYSTEM DESIGN MODEL DETAILS (CONTINUED)

Input Parameters (Yellow)

Salt mdot	11.75	kg/s
**Needed salt mdot	11.75	kg/s over X h
salt node dT transition	20	

Output Parameters (Green)

sCO2 dP goal	1.0-0.9	MPa		
HCHX annulus ID	3.45	m		
Actual stored E	215619	MJ		
Actual stored E	59.9	MW-h		
Goal stored E	60.0	MW-h		
Actual total power	5.0	MW		
Goal total power	5.0	MW		
Actual salt cold temp	290.5	C		
Goal salt cold temp	290	C		
sCO2 inlet temp	265.5	C		
Goal sCO2 inlet temp	>475	C		
flow rate of salt in TC	0.6419	mm/s		
Driving dP	47.7	kPa	6.92	psig
Pressure loss	0.136	kPa	0.02	psig